

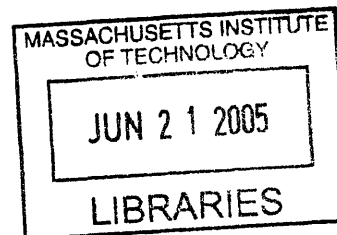
Mechanistic Studies on Palladium-Catalyzed Carbon-Nitrogen Bond

Forming Reactions

by

Liane M. Klingensmith

B.A. Chemistry
Alfred University, 2003

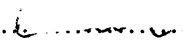


SUBMITTED TO THE DEPARTMENT OF CHEMISTRY IN PARTIAL
FULFILLMENT OF THE REQUIREMENT FOR THE DEGREE OF

SCIENCE MASTERS IN ORGANIC CHEMISTRY
AT THE
MASSACHUSETTS INSTITUTE OF TECHNOLOGY

JUNE 2005

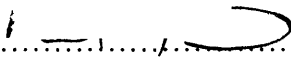
© Massachusetts Institute of Technology, 2005
All rights reserved

Signature of Author:..........

Department of Chemistry
May 20, 2005

Certified by:.....

Stephen L. Buchwald
Camille Dreyfus Professor of Chemistry
Academic Advisor

Accepted by:..........

Robert W. Field
Chairman, Department Committee on Graduate Students

ARCHIVES

Mechanistic Studies on Palladium-Catalyzed Carbon-Nitrogen Bond Forming Reactions

by

Liane M. Klingensmith

Submitted to the Department of Chemistry on May 20, 2005 in Partial Fulfillment of the Requirements for the Degree of Master of Science in Chemistry

ABSTRACT

Precatalyst species present in a solution of $\text{Pd}_2(\text{dba})_3$ and Xantphos were identified as $\text{Pd}(\text{Xantphos})(\text{dba})$ and $\text{Pd}(\text{Xantphos})_2$ by use of ^{31}P NMR and independent syntheses. $\text{Pd}(\text{Xantphos})_2$ was found to form at high ligand concentrations. To determine whether the formation of this species affected reaction rates, reaction calorimetry was used to explore the rate of the palladium-catalyzed coupling of 4-*t*-butylbromobenzene and morpholine using the ligand Xantphos at varying palladium to ligand ratios. It was found that catalyst activity is dramatically dependent on the concentration of ligand relative to palladium, due to formation of $\text{Pd}(\text{Xantphos})_2$. Two plausible hypotheses for the low activity of $\text{Pd}(\text{Xantphos})_2$ as a precatalyst are (1) a slow rate of dissociation of a ligand from the bis-ligated species, and (2) the high degree of insolubility of $\text{Pd}(\text{Xantphos})_2$. Magnetization transfer experiments were used to probe the rate of dissociation of ligand for the bis-ligated species, and reaction calorimetry experiments were performed using the more soluble *t*-butylXantphos in comparison to Xantphos to determine whether the insolubility of $\text{Pd}(\text{Xantphos})_2$ causes it to have relatively low activity. It was found that solubility is not the main cause for the low activity of $\text{Pd}(\text{Xantphos})_2$, and evidence was given to support the hypothesis that low activity results from the slow dissociation of a ligand from the bis-ligated species.

Thesis Supervisor: Stephen L. Buchwald
Title: Camille Dreyfus Professor of Chemistry

Acknowledgments

I would like to thank the MIT department of chemistry for allowing me to further my education at such a fine institution, with a special thanks to Professor Stephen Buchwald for being my academic advisor during my tenure at MIT. Dr. Eric Strieter is thanked for taking me under his wing, and teaching me much about calorimetry, chemistry, and life. Tim Barder is thanked for crystal structure analysis. Jeff Simpson and the DCIF staff are thanked for assistance with NMR experiments and equipment. The Buchwald lab, in particular M. P. R. and J. R. M. are thanked for intellectual discussions, and the whole lab is thanked for their humor. R. A. A. will be remembered for his unprecedented ability to break things, and P. J. B. for his uncontrollable excitement about chemistry.

I would also like to thank my family, my parents in particular, who support me unconditionally. J. W. B. is thanked for being the most amazing woman I have ever met, and for teaching me early in life to stand up for yourself, and to do what makes you happy.

A. Introduction.

I. Mechanistic Studies on Palladium Catalyzed Carbon-Nitrogen Bond Forming Reactions Using a Catalyst System Based on Pd/Xantphos.

Palladium-catalyzed carbon-nitrogen bond forming reactions have become one of the most important cross-coupling reactions in synthetic organic chemistry. Recently, advances have been made with the development of catalyst systems that exhibit increased selectivity and wide substrate scope.¹ One catalyst system, based on the ligand Xantphos² (Figure 1), has been particularly successful in broadening the substrate scope of this reaction.³ Using a Pd/Xantphos catalyst system, difficult reactions such as the *N*-arylation of both heteroarylamines and amides,^{3e, f, g, 5c} the coupling of amines with *ortho*-functionalized base-sensitive aryl halides,⁴ the amination of aryl nonaflates,³ⁱ and the *N*-arylation of 2-oxazolidinones^{3j} can be accomplished.

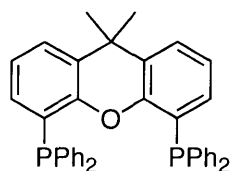


Figure 1 Xantphos.

Although catalyst systems using Xantphos have been utilized for various types of reactions, the reason behind its efficiency is largely unknown.⁵ Van Leeuwen and co-workers initially used Xantphos for palladium catalyzed

amination reactions^{3a} after the observation that other large bite-angle ligands such as DPEphos⁶ worked well. Both Van Leeuwen^{5b} and Buchwald^{5c} have demonstrated that Xantphos can serve as a *trans*-chelating ligand when bound to Pd(II). The bite-angle of Xantphos in these complexes is around 153°, which is much larger than the calculated flexible bite angle (97-135°).⁷ Buchwald suggests that the large bite angle is a result of an interaction between the oxygen atom and palladium, which can be seen in the crystal structure. Additionally, it is possible that a palladium-oxygen interaction causes Xantphos to assume a much larger bite-angle when catalyzing reactions. Buchwald also suggests that in order for reductive elimination to occur from a *trans*-chelating complex, one arm of Xantphos may dissociate from the metal. In support of this, Van Leeuwen has reported that in solution *cis/trans* isomerization can occur^{5b} through a one-arm dissociation event.

Van Leeuwen and co-workers have performed a detailed kinetic analysis of these reactions employing both a (Xantphos)Pd(Ar)Br complex and a cationic (Xantphos)Pd(Ar)OTf complex as precatalysts.^{5a} However, these studies, which are based only on initial rates, may be misleading since recent studies have shown anomalous rate behavior while measuring reaction kinetics under these conditions.^{8b, c}

Our goal was to continue determining the characteristics of Xantphos that allow for increased substrate scope in carbon-nitrogen bond forming reactions. These findings would not only yield mechanistic insight, but would also be helpful

in designing new ligands that could induce better selectivity and substrate scope than is already observed.

II. Reaction Calorimetry

Reaction calorimetry⁸ has proven itself to be an extremely useful method for performing kinetic analysis of multi-step reactions. Classical kinetic measurements involve initial rate studies, “flooding”—using an unusually large excess of one reagent, sampling, and NMR studies. Initial rate studies are particularly misleading in catalytic reactions since in most cases only a limited number of turnovers will be observed. Flooding is also misleading for catalytic and multi-step reactions since this can alter the rate-determining step, and dramatically alter the kinetic profile of the reaction. Sampling of reactions can introduce error, and can be excruciatingly time-consuming. NMR studies have been shown to be very useful if the conditions of the study are such that the reaction mixture is homogeneous and no stirring is needed.

Reaction calorimetry is a non-invasive method that allows the measure of heat flow versus time during the course of a reaction. Reaction calorimetry conditions are considered to be “synthetically relevant” as the reaction can be performed in a vessel under the exact same conditions it would be performed if no kinetic analysis were being performed.

The heat flow (q) measured during the course of a reaction is proportional to the reaction rate, r , where ΔH_{rxn} is the heat of reaction and V is the reaction volume (Equation 1).

$$q = \Delta H_{\text{rxn}} Vr$$

Equation 1

The heat flow measurements can be used to calculate percent conversion of starting material at any point during the reaction by dividing the area of all heat flow measurements up to any time point t by the sum of the heat flow for the entire duration of the reaction t_f (Equation 2).

$$\text{fractional conversion} = \frac{\int_{t_0}^t q(t) dt}{\int_{t_0}^{t_f} q(t) dt}$$

Equation 2

Reaction calorimetry was used to study palladium-catalyzed carbon-nitrogen bond forming reactions using Xantphos and *t*-butylXantphos as supporting ligands, and $\text{Pd}_2(\text{dba})_3$ as the palladium source.

B. Results and Discussion

The palladium-catalyzed coupling of 4-*t*-butylbromobenzene and morpholine (Figure 2) was used in calorimetry studies due to its rapid reaction rate and the high conversion of the aryl bromide. A vial containing Pd₂(dba)₃, Xantphos, NaOt-Am, 1,4-dioxane, and toluene⁹ was equilibrated at 60 °C for 1 h. Morpholine and 4-*t*-butylbromobenzene were injected after equilibration to initiate the reaction. A sample reaction calorimetry kinetic analysis, which shows fractional conversion vs. time, is also shown in Figure 2. In order to verify that heat flow measurements correspond to conversion of starting material to product, a GC correlation is performed by measuring conversion of starting material at various time points in separate reactions by GC, and plotting those points on top of the calorimetric fractional conversion vs. time plot. The two plots are consistent, i.e., the measured heat flow is due to product formation, and calorimetry is an accurate technique to observe heat flow in this reaction.

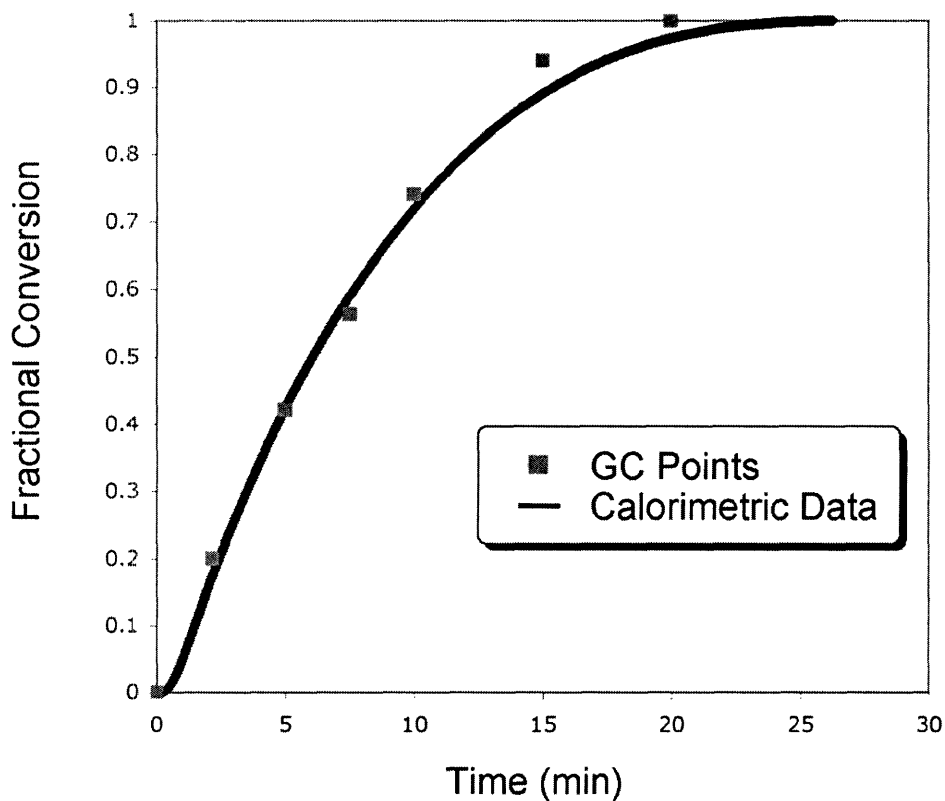
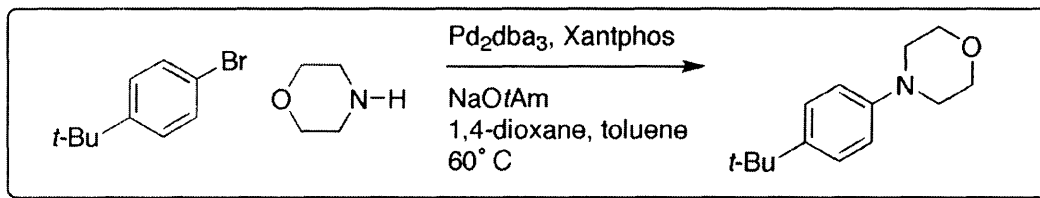


Figure 2 Fraction Conversion vs. Time for Calorimetric and GC Data. $[\text{ArBr}]_0 = 0.25 \text{ M}$; $[\text{Amine}]_0 = 0.30 \text{ M}$ (1.2 equivalents); $[\text{NaOtAm}]_0 = 0.35 \text{ M}$ (1.4 equivalents; 1:1 Xantphos/Pd from $\text{Pd}_2(\text{dba})_3$ 2.5 mol % Pd based on ArBr; 1,4-Dioxane 3 ml, Toluene 1 ml⁹.

Our initial studies revealed that the palladium to ligand ratio has a dramatic effect on reaction rate, as shown in Figure 3. It was found that for the simple reaction we were studying, a ligand to palladium ratio of 1:1 is optimal, and that at higher ligand concentrations, the reaction rate dramatically decreases. One possible hypothesis is that at high ligand ratios the

concentration of active catalyst is suppressed by formation of a less active species. In order to test this hypothesis, information was needed about the structure of the precatalyst.

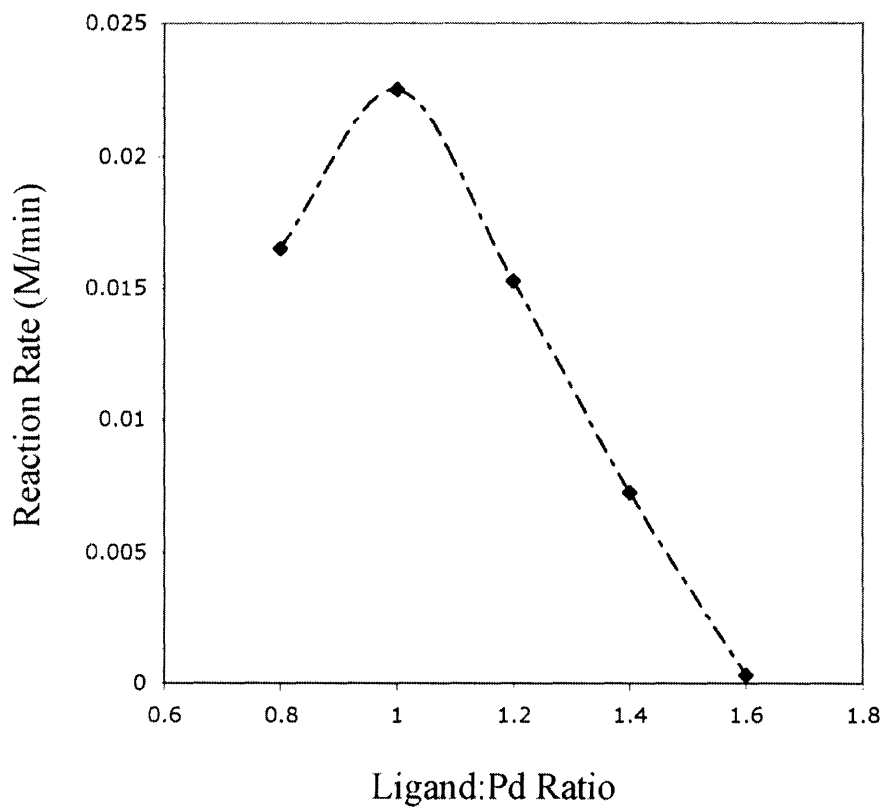
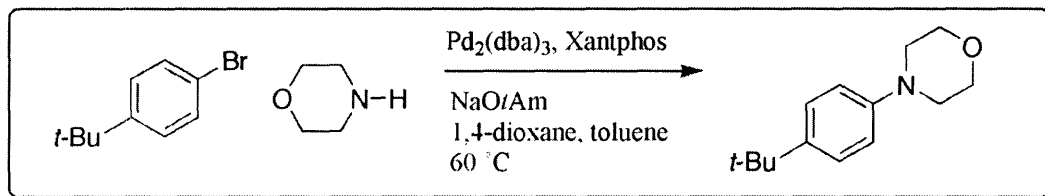


Figure 3 Reaction Rate vs. Ligand: Pd Ratio. $[\text{ArBr}]_0 = 0.25 \text{ M}$; $[\text{Amine}]_0 = 0.30 \text{ M}$ (1.2 equivalents); $[\text{NaOtAm}]_0 = 0.35 \text{ M}$ (1.4 equivalents); $\text{Pd}_2(\text{dba})_3$ 2.5 mol % Pd based on ArBr; Xantphos 2 mol % - 4 mol % based on ArBr; 1,4-Dioxane 3 ml, Toluene 1 ml. Reaction rate is at 10 % conversion of ArBr.

We wanted to determine what species are present in a solution of Xantphos and $\text{Pd}_2(\text{dba})_3$. This knowledge would allow for structural information about the precatalyst, and also could determine the cause of the rate decrease at higher Xantphos concentrations. There are several species which are likely to form in a solution of Xantphos and $\text{Pd}_2(\text{dba})_3$, some of which are shown in Figure 4.

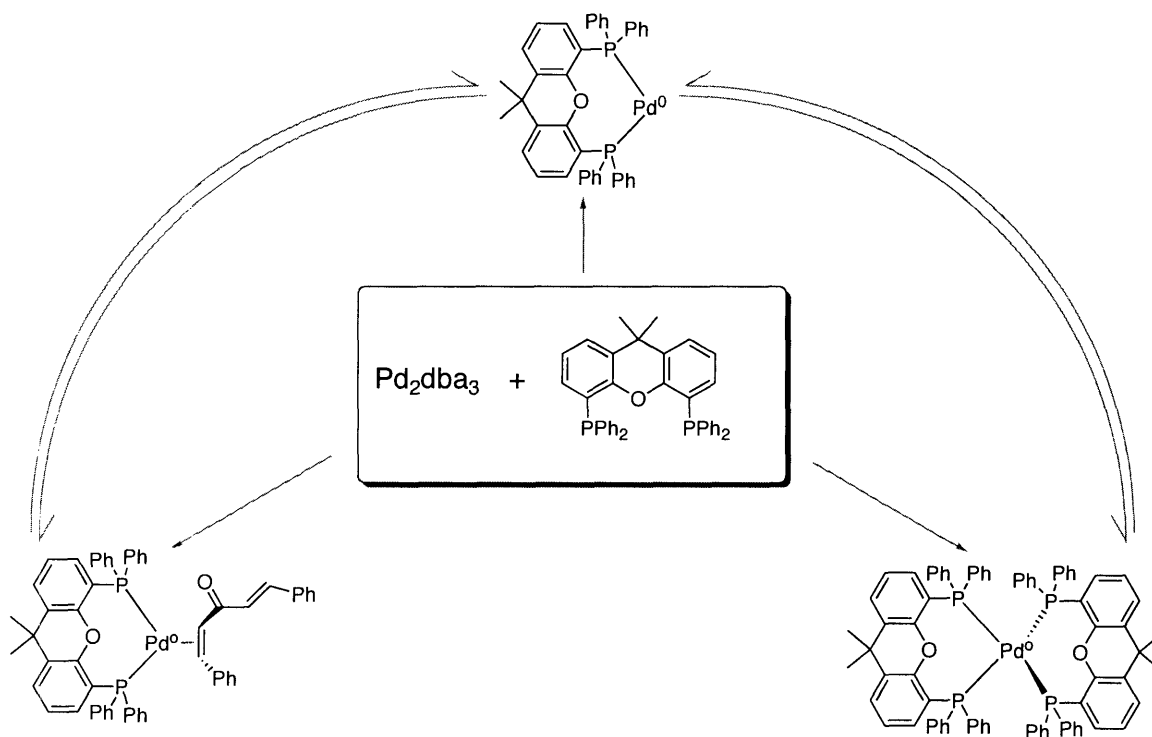


Figure 4 Species which are likely formed when Xantphos and $\text{Pd}_2(\text{dba})_3$ are mixed.

A common and useful method for studying palladium-phosphine complexes is ^{31}P NMR. We wanted to determine the quantity of species present,

and then to identify these species. However, due to the low solubility of Xantphos and $\text{Pd}_2(\text{dba})_3$, NMR experiments could not be conducted. To avoid this problem, initial studies were conducted using the more soluble *t*-butylXantphos (Figure 5).¹⁰

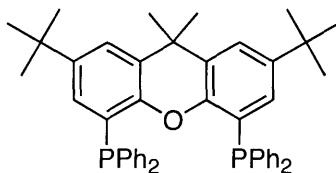


Figure 5 *t*-butylXantphos

$\text{Pd}_2(\text{dba})_3$ and *t*-butylXantphos (1:1 L: Pd) were stirred in toluene at room temperature under inert atmosphere for two hours. This orange-red solution was filtered through a glass frit inside of a glovebox to remove insoluble matter. After concentrating this solution slightly, ^{31}P NMR experiments were performed at variable temperatures. As shown in Figure 6, at least two different species were present. Species B has a complex splitting pattern at low temperatures, and starts to coalesce to one peak at higher temperatures. The other two peaks, labeled as Species A, may be consistent with two inequivalent phosphorous atoms on one palladium atom.

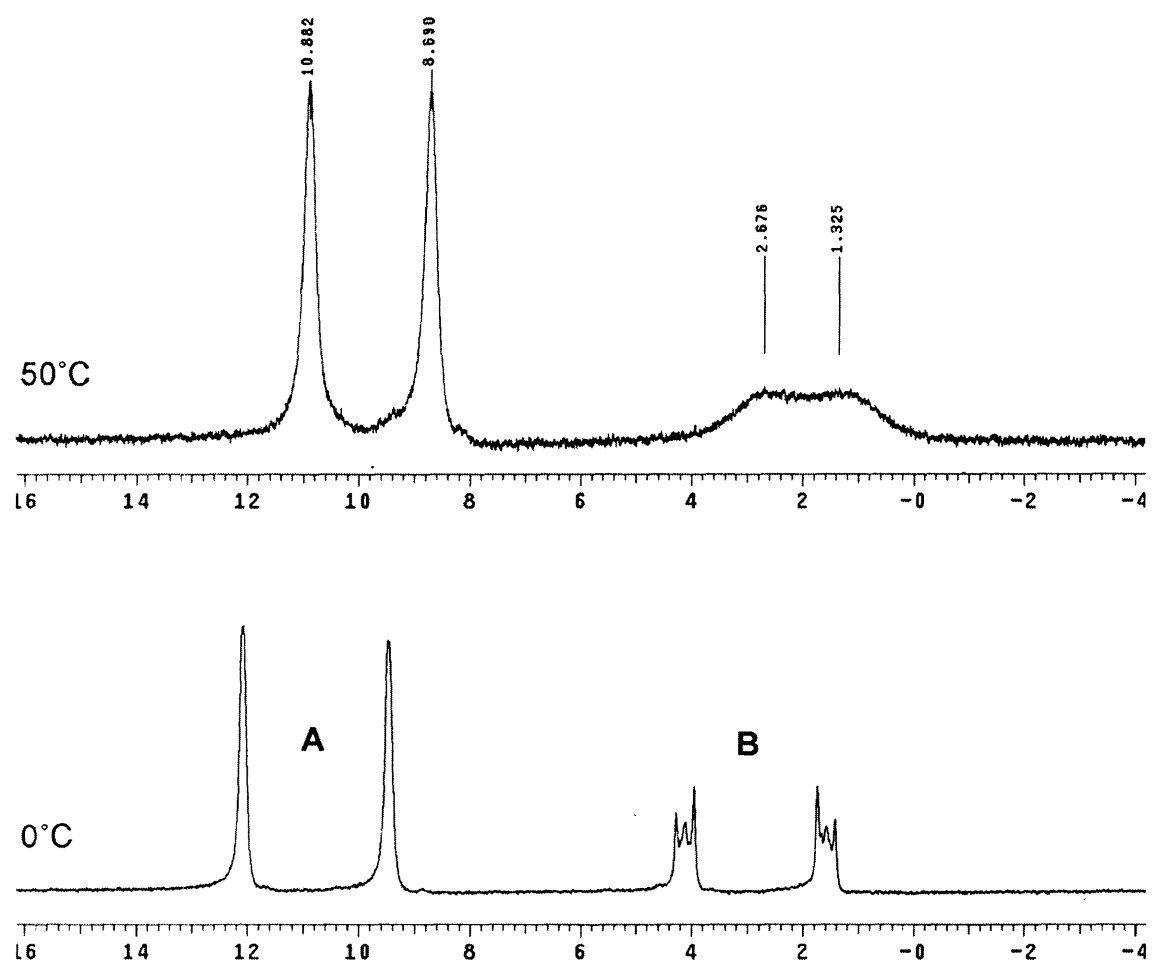
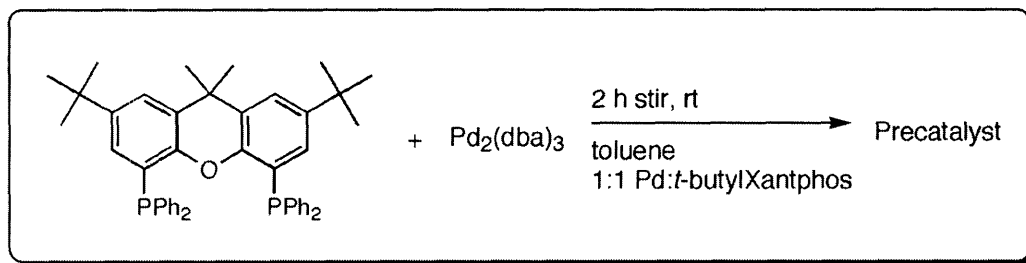


Figure 6 ^{31}P NMR of precatalyst at different temperatures.

In order to identify these peaks, complexes composed of palladium, *t*-butylXantphos, and dibenzylidene acetone were separately synthesized as shown in Figure 7.

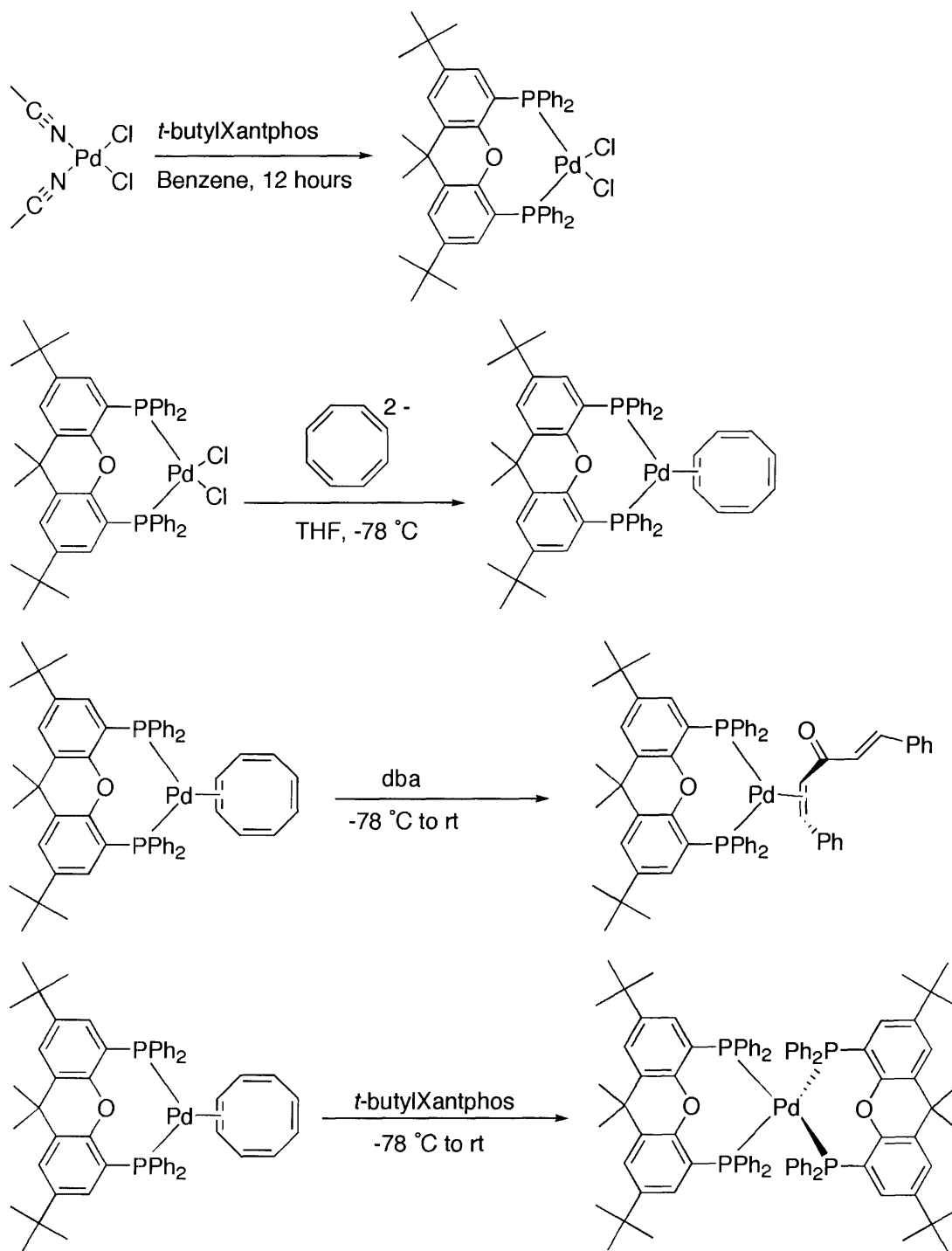


Figure 7 Synthesis of palladium-*t*-butylXantphos complexes.

$\text{PdCl}_2(t\text{-butylXantphos})$ was synthesized using an analogous procedure to synthesize $\text{PdCl}_2(\text{dppf})$.¹¹ Using the straightforward route to bisphosphine-cyclooctatetraene Pd(0) complexes developed by Brown and Cooley,¹² $t\text{-butylXantphos-cyclooctatetraene Pd(0)}$ was synthesized from the above described $\text{PdCl}_2(t\text{-butylXantphos})$ complex. Cyclooctatetraene is an extremely labile ligand and can be displaced easily from a metal center with another alkene or phosphine ligand. In this way, both $\text{Pd}(t\text{-butylXantphos})(\text{dba})$ ¹³ and $\text{Pd}(t\text{-butylXantphos})_2$ were synthesized; the ³¹P NMR spectra are shown in Figure 8.

$\text{Pd}(t\text{-butylXantphos})(\text{dba})$ corresponds to the two large peaks around $\delta_{\text{P}} 9.8$ and $\delta_{\text{P}} 12.4$ ppm. The two phosphorous atoms on palladium are inequivalent due to the non-symmetric bonding of dba on palladium, which accounts for the P-P coupling observed. The phosphorous atoms in $\text{Pd}(t\text{-butylXantphos})_2$ resonate around $\delta_{\text{P}} 0.8$ and $\delta_{\text{P}} 3.4$ ppm (in THF). As shown above in Figure 6, the ³¹P NMR of this complex at 0 °C exhibits a complex splitting pattern, which suggests that this complex does not possess tetrahedral symmetry.

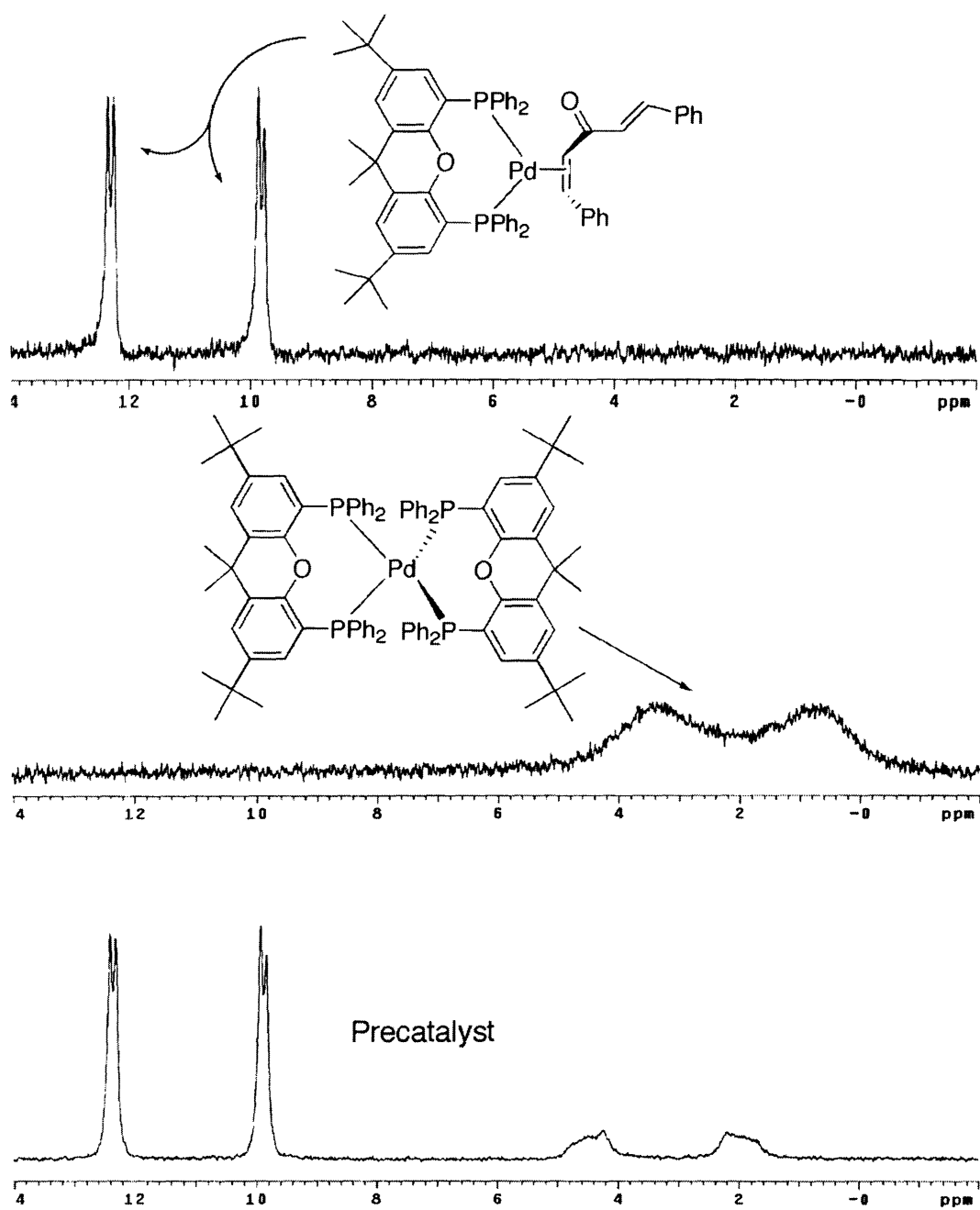


Figure 8 ^{31}P NMR analysis of palladium complexes made from Pd(*t*-butylXantphos)(cyclooctatetraene). Pd(*t*-butylXantphos) $_2$ and Pd(*t*-butylXantphos)(dba) are in THF, precatalyst is in toluene.

An X-ray quality crystal of $\text{Pd}(t\text{-butylXantphos})_2$ ¹⁵ was grown by synthesizing the complex by the route shown in Figure 7, dissolving the product in benzene, and finally layering with ether. The ORTEP diagram is shown in Figure 9a. However, this complex is extremely crowded and to allow for better interpretation, the phenyl groups have been removed for clarity (Figure 9b). The complex exists in the solid state as a distorted tetrahedron, with P-Pd bond lengths: 2.3809(13), 2.3857(12), 2.3846(14), 2.4001(14) Å, and P-Pd-P angles: 108.07(4), 108.73(5), 113.51(4), 108.09(4), 109.40(5), 108.90(5)°. The Pd-P bond length of 2.4001(14) Å is slightly longer than other Pd-P bond lengths, and the angle of 113.51(4)° is considerably larger than the other angles, which may account for the complex splitting pattern observed by ³¹P NMR at 0 °C (Figure 6). In solution at room temperature, the complex splitting pattern is no longer observed, meaning that the solution state structure is highly fluxional.

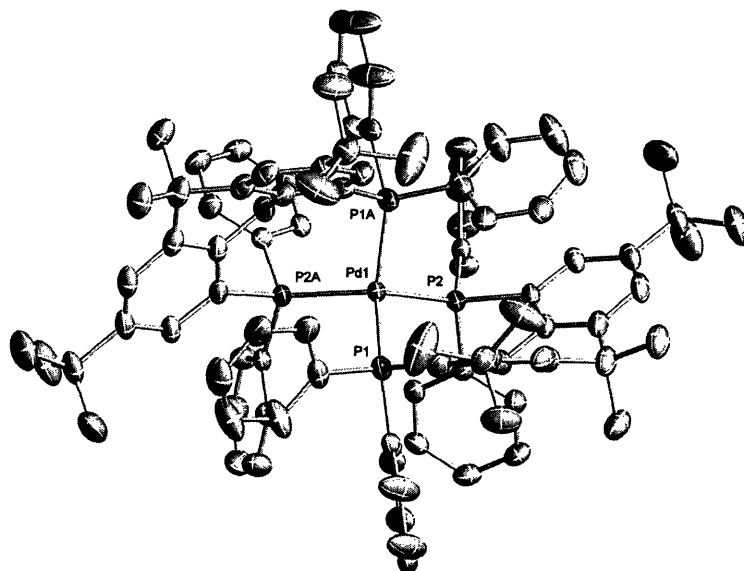


Figure 9a. ORTEP diagram of *t*-butylXantPhos₂Pd with hydrogen atoms, benzene molecule and ether molecule removed for clarity. Thermal ellipsoids are at 30% probability.

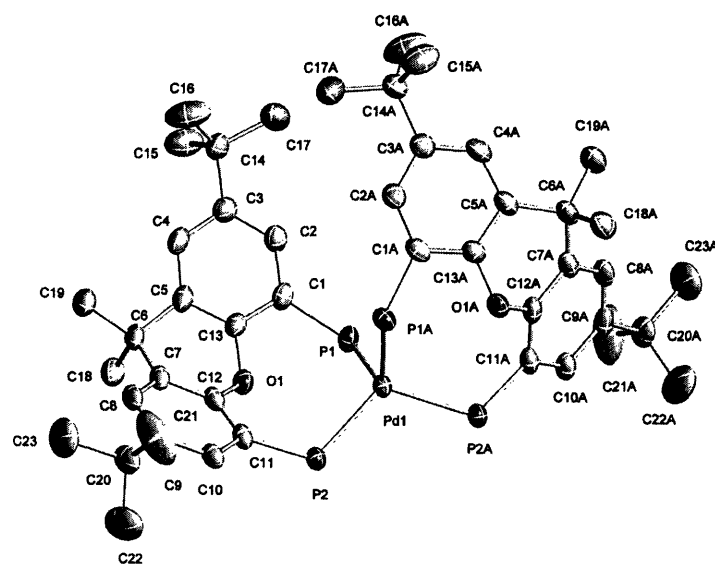


Figure 9b. ORTEP digram of *t*-butylXantPhos₂Pd with hydrogens, phenyl groups, benzene molecule and ether molecule removed for clarity. Thermal ellipsoids at 30% probability.

Although all of these studies were performed with *t*-butylXantphos, it is likely that the corresponding species also form when employing Xantphos. As a dramatic rate decrease is observed at high Xantphos concentrations, we wanted to determine what causes this phenomenon. As was expected, stirring an excess of *t*-butylXantphos (3:1 L: Pd) and Pd₂(dba)₃ in toluene produced a ³¹P NMR with Pd(*t*-butylXantphos)₂ as the predominant species (Figure 10). This observation suggests that the corresponding Pd(Xantphos)₂ species forms at higher Xantphos concentrations. Such an experiment was attempted with Xantphos; however, an insoluble yellow/green precipitate formed, making analysis by NMR impossible.

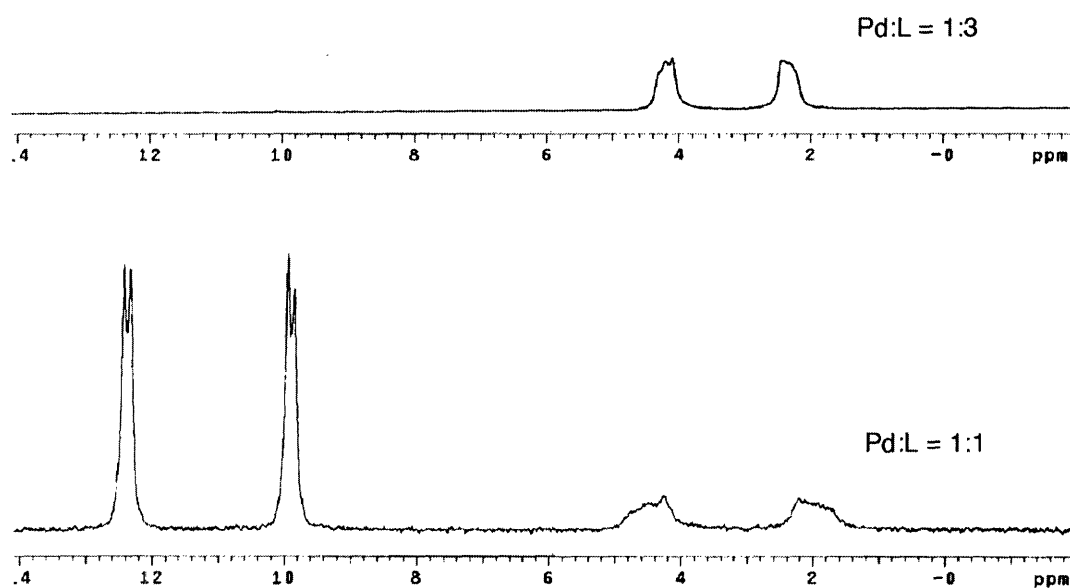
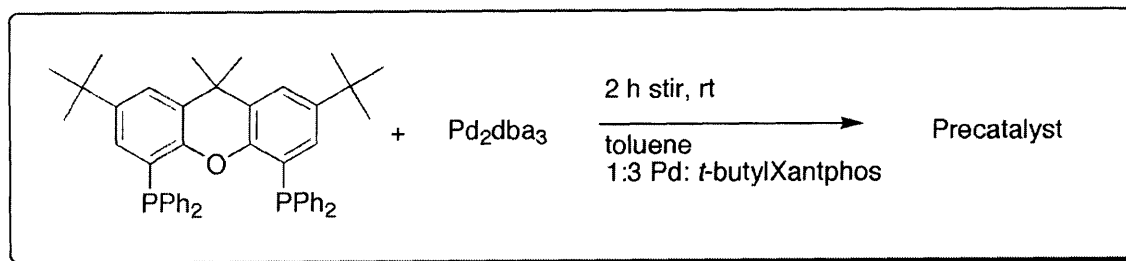


Figure 10 Precatalyst Mixture of Pd:L 1:3 vs. Pd:L 1:1

Although NMR experiments could not be conducted with Xantphos, Pd(Xantphos)₂ could be isolated. Xantphos and Pd₂(dba)₃ were stirred in an extremely dilute solution of toluene (0.002 M based on Pd). The solution was filtered to remove palladium black, concentrated slightly, filtered again, and finally concentrated completely. At this point, the yellow solid¹⁶ was trituated in toluene overnight to remove dibenzylidene acetone and excess Xantphos. The resulting yellow solid is sparingly soluble in common organic solvents. The identity of the

species was confirmed to be Pd(Xantphos)₂ by use of MALDI-TOF-MS analysis and elemental analysis.

From these NMR experiments, it is believed that when Pd(Xantphos)₂ forms in a catalytic reaction, the reaction rate decreases significantly. Others have reported trends that can account for the formation of this species. Buchwald and co-workers reported “an unusual dependence on catalyst loading,” where the reactions being studied were more efficient at lower catalyst concentrations.^{5c} Another observation is that difficult reactions employing Xantphos are often run at very low concentrations (0.25–0.13 M),^{3g, 4} which would minimize the formation of Pd(Xantphos)₂.

Due to the insolubility of Pd(Xantphos)₂, it was our hypothesis that catalyst deactivation occurs at high Xantphos concentrations, i.e. this inactive species forms, and precipitates from solution. An alternative hypothesis is that an equilibrium exists between the bis-ligated species and the mono-ligated palladium species in solution, and this equilibrium lies towards the bis-ligated species (Figure 11).

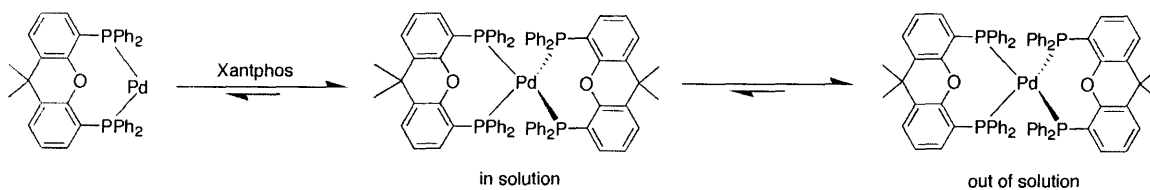


Figure 11 Equilibrium of palladium-Xantphos species.

To test these hypotheses, experiments were performed at varying ligand to palladium ratios with both Xantphos and *t*-butylXantphos. The results of these studies are shown in Figure 12.

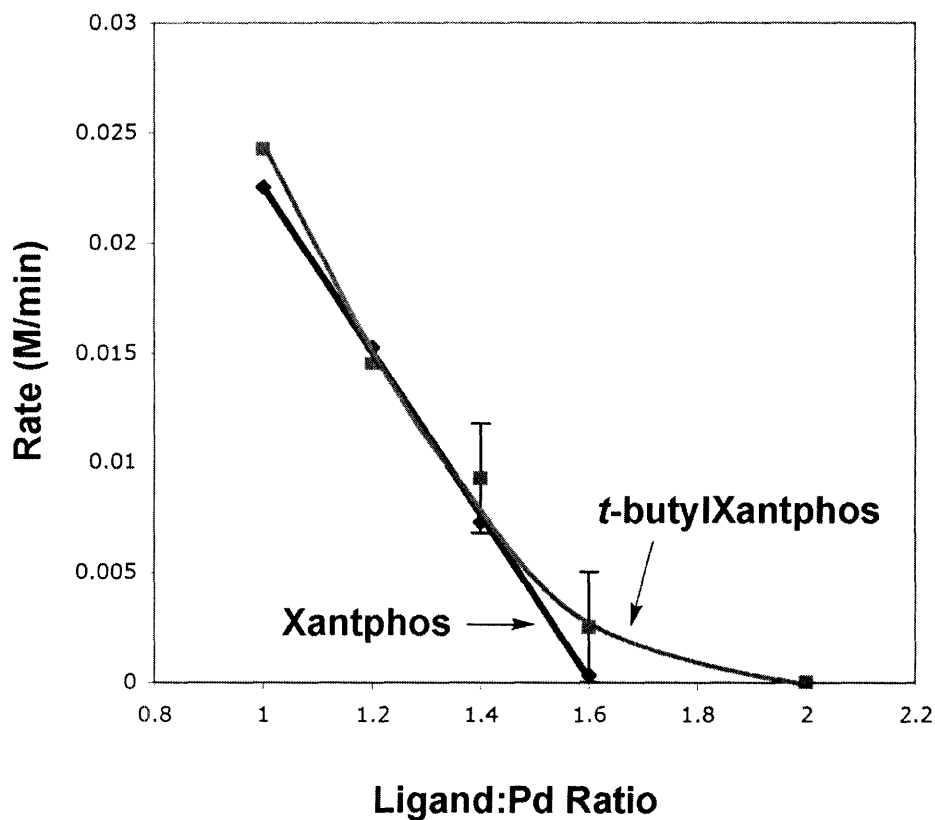
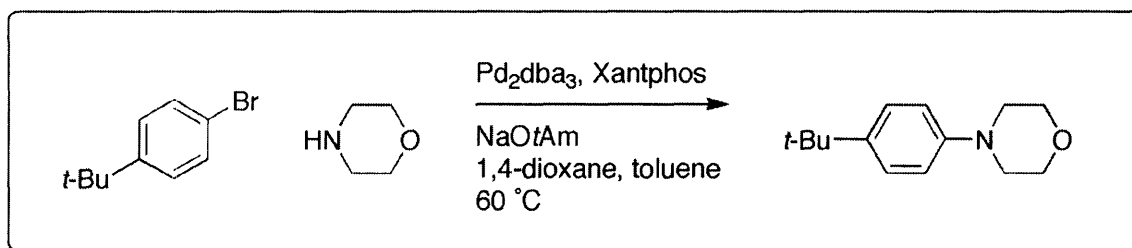


Figure 12 Plot of Rate vs. Ligand:Palladium Ratio for both Xantphos and *t*-butylXantphos. $[\text{ArBr}]_0 = 0.25 \text{ M}$; $[\text{Amine}]_0 = 0.30 \text{ M}$ (1.2 equivalents); $[\text{NaOtAm}]_0 = 0.35 \text{ M}$ (1.4 equivalents); $\text{Pd}_2(\text{dba})_3$ 2.5 mol % Pd based on ArBr; Ligand 2 mol % - 4 mol % based on ArBr; 1,4-dioxane 3 ml, toluene 1 ml.⁹

At high ligand to palladium ratios (>1.6), *t*-butylXantphos continues to catalyze the reaction, whereas the reaction with Xantphos provides no product. However, at ligand to palladium ratios between 1 and 1.6, the rate profiles are essentially identical for Xantphos and *t*-butylXantphos.

To further test the hypothesis that the solubility of Pd(Xantphos)₂ can cause catalyst deactivation, reactions were catalyzed by employing Pd(Xantphos)₂ and Pd(*t*-butylXantphos)₂ as precatalysts. Rate versus fractional conversion is shown in Figure 13a, and rate versus time is shown in Figure 13b for the coupling of *p*-*t*-butylbromobenzene and morpholine.

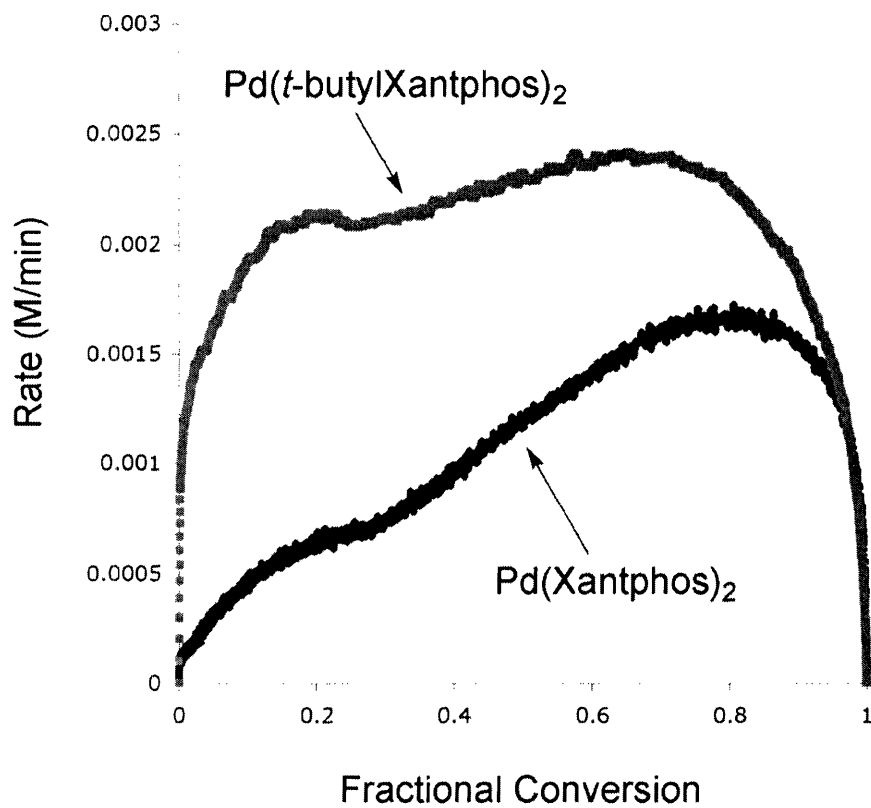
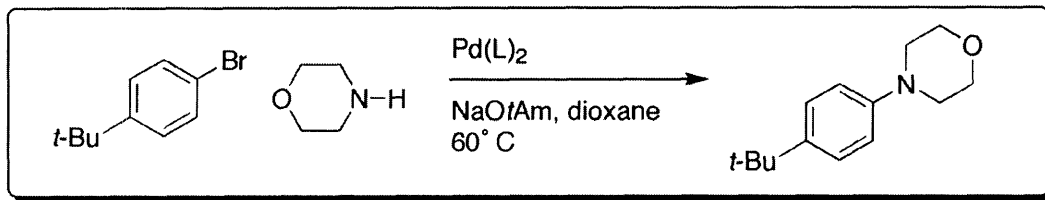


Figure 13a Reaction Rate vs. Fractional Conversion for reactions catalyzed by $\text{Pd}(t\text{-butylXantphos})_2$ and $\text{Pd}(\text{Xantphos})_2$ $[\text{ArBr}]_0 = 0.25\text{ M}$; $[\text{Amine}]_0 = 0.30\text{ M}$ (1.2 equivalents); $[\text{NaOtAm}]_0 = 0.35\text{ M}$ (1.4 equivalents); 2.5 % Pd(L)_2 based on $[\text{ArBr}]$; 1,4-dioxane, 4 ml.

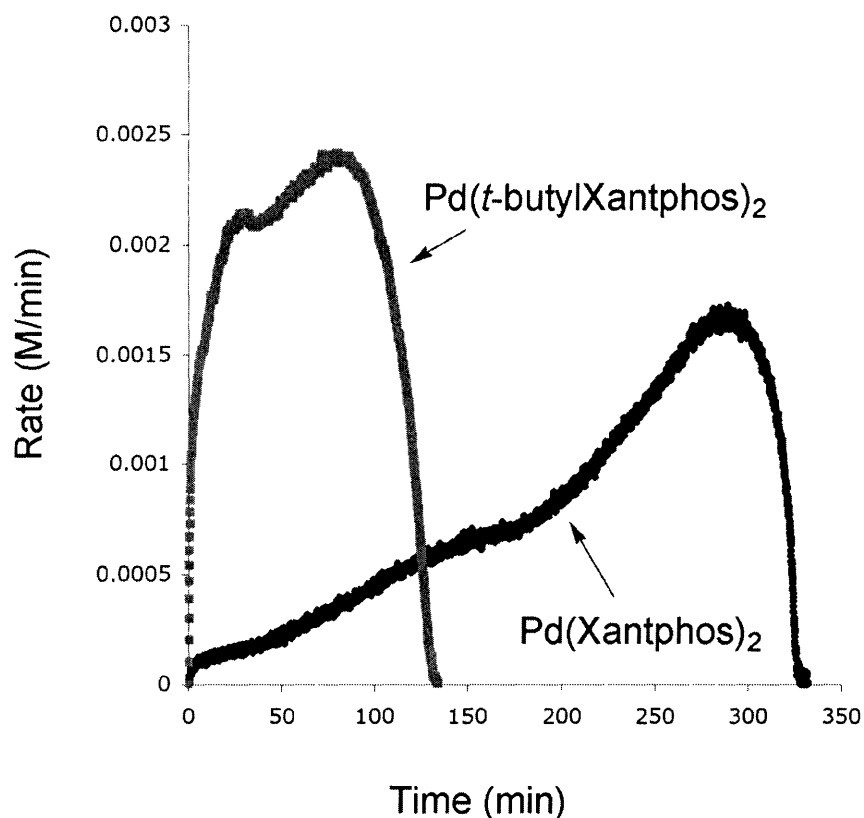
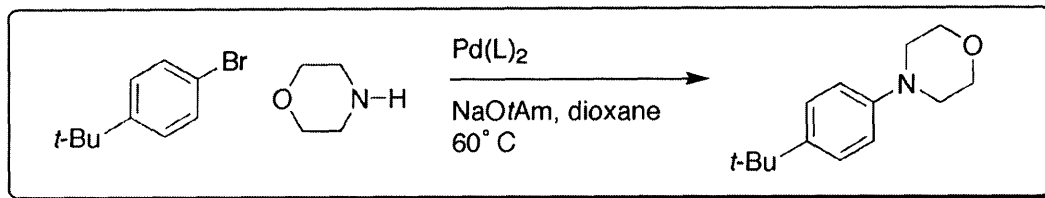


Figure 13b Reaction Rate vs. Time for reactions catalyzed by $\text{Pd}(t\text{-butylXantphos})_2$ and $\text{Pd}(\text{Xantphos})_2$ [$\text{ArBr}]_0 = 0.25\text{ M}$; [$\text{Amine}]_0 = 0.30\text{ M}$ (1.2 equivalents); [$\text{NaOtAm}]_0 = 0.35\text{ M}$ (1.4 equivalents); 2.5 % Pd(L)_2 based on [ArBr]; 1,4-dioxane, 4 ml.

The reaction catalyzed by $\text{Pd}(\text{Xantphos})_2$ exhibits a very interesting kinetic profile in that the rate is slowly increasing throughout the reaction. This can be compared to the kinetic profile of the corresponding reaction in which $\text{Pd}(t\text{-butylXantphos})_2$ is the precatalyst. In this reaction, the rate is generally the same

throughout the reaction, exhibiting zero-order kinetics. This is very similar to an observation of zero-order kinetics made both by van Leeuwen and co-workers^{5a} and by Hartwig and co-workers^{ref} while studying palladium-catalyzed carbon-nitrogen bond formation using Pd/Xantphos and Pd/BINAP catalyst systems, respectively. Buchwald and Blackmond^{8a} later demonstrated that the zero order dependence on substrate may arise from the slow rate of active catalyst formation. This would be the case if a slow dissociation of *t*-butylXantphos from Pd(*t*-butylXantphos)₂ was occurring. This slow dissociation is also occurring from Pd(Xantphos)₂; however, along with this dissociation is a slow equilibration allowing more precatalyst into solution, which accounts for the increasing rate of reaction.

Attempts were made using a ³¹P NMR magnetization transfer experiment to measure the rate of dissociation of a ligand from the bis-ligated species (Figure 14); a procedure which has been reported before by Grubbs and co-workers.¹⁷ To do this, a solution containing Pd(*t*-butylXantphos)₂ and *t*-butylXantphos (1.0:1.5 ratio) in benzene-*d*₆ was equilibrated in an NMR probe, and then the free ligand was selectively inverted using a 180° pulse. After variable mixing times between 0.0100 and 5.12 s, a nonselective 90° pulse was applied. Using this method, if free ligand were to exchange rapidly enough with complexed ligand, the peak area for the complex would decrease following exchange with the inverted signal of the free ligand. Even at 60 °C, however, no change in the integral values was observed, meaning that no appreciable

exchange (or less exchange than is capable of being detected by NMR) was occurring between the complexed and free ligand.

This method is only useful for rates of exchange that are large enough relative to (1) the relaxation rate of the complexed ligand, and (2) the relaxation rate of the free ligand. That is, the rate of magnetization loss due to exchange of the complexed ligand with free ligand must be large enough to measure before the NMR signal of the complexed ligand returns to equilibrium and/or the before the free ligand relaxes back to equilibrium following selective inversion. We found that in this case, the rate of exchange is too slow to measure before relaxation occurs, and a binding constant could not be obtained. This data suggests that the binding constant is very large for $\text{Pd}(t\text{-butylXantphos})_2$, meaning that the reason for its inefficiency as a precatalyst is likely the slow formation of the active mono-ligated species (Figure 14).

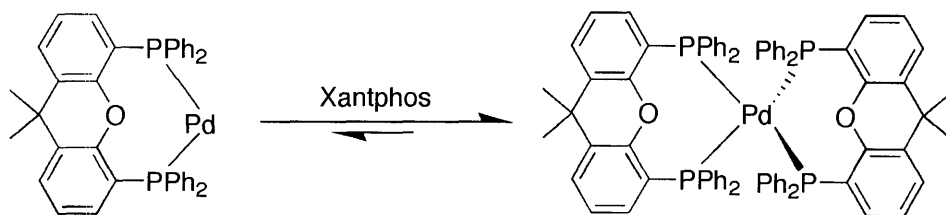


Figure 14 Equilibrium between mono and bis-ligated Xantphos-palladium species.

C. Conclusions

Products from mixing Xantphos and $\text{Pd}_2(\text{dba})_3$ were identified as $\text{Pd}(\text{Xantphos})_2$ and $\text{Pd}(\text{Xantphos})(\text{dba})$. This was accomplished by separately synthesizing the analogous *t*-butylXantphos species, and comparing their ^{31}P NMR spectra to the ^{31}P NMR spectrum of a mixture of *t*-butylXantphos and $\text{Pd}_2(\text{dba})_3$. $\text{Pd}(\text{Xantphos})(\text{dba})$ serves as the precatalyst and $\text{Pd}(\text{Xantphos})_2$ demonstrates extremely low activity as a precatalyst.

Reaction rates were essentially the same for reactions catalyzed by Xantphos and *t*-butylXantphos at ligand:Pd ratios between 1.0 and 1.5, meaning that the insolubility of $\text{Pd}(\text{Xantphos})_2$ is not the cause of its low activity, since $\text{Pd}(\textit{t}\text{-butylXantphos})_2$ is completely soluble. Furthermore, it was demonstrated through reaction calorimetry that $\text{Pd}(\text{Xantphos})_2$ is in equilibrium with $\text{Pd}(\text{Xantphos})$ by use of $\text{Pd}(\text{Xantphos})_2$ as the precatalyst. The size of this equilibrium was probed by use of a magnetization transfer experiment, and it was found that formation of $\text{Pd}(\text{Xantphos})_2$ in the palladium-catalyzed amination of 4-*t*-butylbromobenzene significantly decreases the rate of reaction, not due to solubility, but due to a very large binding constant for ligand on the bis-ligated species which causes a slow generation of mono-ligated active catalyst.

D. Experimental

Reagents. Toluene and THF were purchased from J. T. Baker in CYCLE-TAINER[®] solvent delivery kegs and vigorously purged with argon for 2 h. The solvent was further purified by passing it under argon pressure through two packed columns of neutral alumina (THF) or through neutral alumina and copper (II) oxide (toluene). 1,4-Dioxane, benzene, and morpholine were purchased from Aldrich Chemical Co. in SureSeal containers and taken into a glovebox before use. Xantphos, dichlorobis(acetonitrile)palladium (II), tris(dibenzylideneacetone)dipalladium(0), and lithium granules were acquired from Strem Chemicals, Inc. and used without further purification. 1-Bromo-4-*tert*-butylbenzene was purchased from Aldrich Chemical Co. and distilled from CaH₂ prior to use. Sodium *tert*-amylate (NaOtAm), purchased from Aldrich, was stored and used inside of the glovebox. 4,5-dibromo-2,7-di-*tert*-butyl-9,9-dimethylxanthene, *n*-BuLi (2.5 M in SureSeal bottle), and cyclooctatetraene were purchased from Aldrich Chemical Co. and used without further purification. Chlorodiphenylphosphine (98%) was purchased from Strem Chemical Co. and distilled over CaH₂ under reduced pressure prior to use. All reagents used in reaction calorimetry experiments were handled and stored in a nitrogen-filled glovebox, except for tris(dibenzylideneacetone)dipalladium(0), which was weighed in air into a septum-sealed vial. This vial was then evacuated/backfilled with argon three times before it was taken into a glovebox.

Analytical Methods. ^1H NMR spectra were obtained either on a Bruker 400 MHz, or a Varian Mercury 300 MHz spectrometer, with chemical shifts reported with respect to residual solvent peaks. $^{31}\text{P}\{^1\text{H}\}$ NMR spectra were obtained either on a Varian 500 MHz, or Varian Mercury 300 MHz, with chemical shifts reported with respect to calibration with an external standard of phosphoric acid (0 ppm). MALDI-TOF was performed on a Bruker Omnixflex calibrating externally with a ProteoMass™ Peptide MALDI-MS Calibration Kit. Melting points (uncorrected) were obtained on a Mel-Temp capillary melting point apparatus. Gas Chromatographic analyses were performed on a Hewlett-Packard 6890 gas chromatography instrument with an FID detector using 25m x 0.20 mm capillary column with cross-linked methyl siloxane as a stationary phase. Elemental Analyses were obtained from Atlantic Microlab, Inc. (Norcross, Georgia).

Reaction Calorimetry Experimental Details. Reactions were performed in either an Omnical SuperCRC or an Omnical Reactmax reaction calorimeter. The instrument contains an internal magnetic stirrer and a differential scanning calorimeter (DSC), which compares the heat released or consumed in a sample vessel to an empty reference vessel. The reaction vessels were 16 mL borosilicate screw-thread vials fit with open-top black phenolic screw caps and white PTFE septa (KimbleBrand) charged with Teflon-coated stir bars. Sample volumes did not exceed 4.2 mL. A stock solution of Xantphos or *t*-butylXantphos was made by dissolving 0.250 mmol ligand (145 mg Xantphos, 173 mg *t*-butylXantphos) in 5.00 mL toluene in a volumetric flask to make a 0.0500 M

solution. $\text{Pd}_2(\text{dba})_3$ was weighed in air and brought into the glovebox by evacuating and backfilling a small vial with argon three times. 1 mL of dioxane was then added and stirred to form a slurry. This slurry was then added to the previously weighed NaOtAm in the reaction vessel. The desired amount of ligand was added by taking a portion of the stock solution and diluting to a total volume of 1.0 mL in toluene, so that each reaction contained a constant amount of toluene with varying amounts of ligand (i.e., If 0.025 mmol ligand was desired, 0.50 mL of the stock solution was delivered to a vial and 0.50 mL toluene was added. If 0.03 mmol ligand was desired, 0.60 mL of the stock solution was delivered to a vial, and 0.40 mL of toluene was added.) This solution of ligand was added to the calorimeter vial containing the NaOtAm and $\text{Pd}_2(\text{dba})_3$, and finally 2.0 mL of dioxane was added and the reaction vessel was sealed. This vessel was then removed from the glovebox and placed in the calorimeter and stirred for one hour, allowing the contents of the vessel to reach thermal equilibrium. Simultaneously, a syringe containing 1-bromo-4-*tert*-butylbenzene and morpholine was placed in the sample injection port of the calorimeter, and was allowed to thermally equilibrate. The reaction was initiated by injecting the mixture of aryl bromide and amine into the stirred catalyst- NaOtAm solution. The temperature of the DSC was held constant at 333K using the internal temperature controller in the calorimeter, ensuring that the reaction would proceed under isothermal conditions. A raw data curve was produced by measuring the heat flow from the sample vessel every six seconds during the reaction. Due to the delay between the instantaneous heat flow being evolved

from the reaction vessel, and the time the thermophile sensor detects the heat flow, the raw data curve must be calibrated. To accomplish this calibration, a constant amount of current was passed through a resistor in the sample chamber of the calorimeter thereby producing a known quantity of heat. This process results in a response curve, which is then transformed into a square wave allowing for the response time of the instrument to be calculated using the WinCRC software. Application of the response time to the raw data results in a “tau corrected data curve.” The tau corrected data curve is a plot of heat flow (mJ s⁻¹) versus time. The reaction rate, which is directly proportional to the heat flow (Equation 1), fractional conversion (Equation 2), and instantaneous concentrations of reactants/products can all be calculated from this tau corrected data curve.

$$q = \Delta H_{rxn} V r$$

Equation 1

$$\text{fractional conversion} = \frac{\int_{t_0}^t q(t) dt}{\int_{t_0}^{t_f} q(t) dt}$$

Equation 2

As a control, the conversion measured by GC analysis was compared to conversion measured by heat flow (Figure 15). Agreement between the two

curves suggests that calorimetric analysis was a valid method for studying rates of this type of reaction.

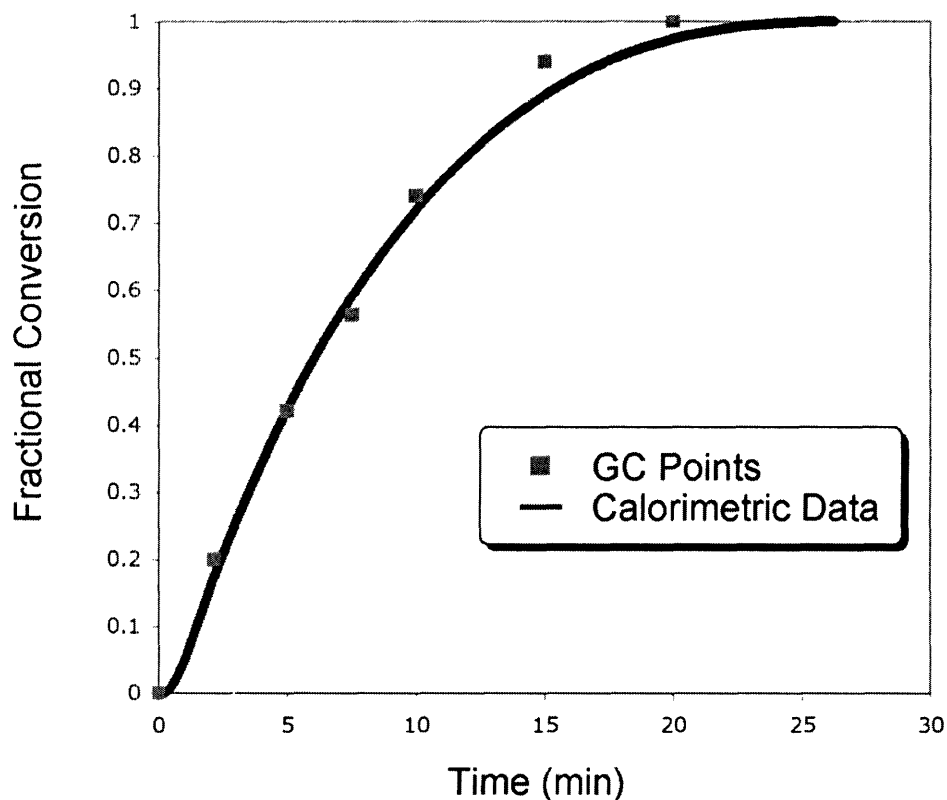
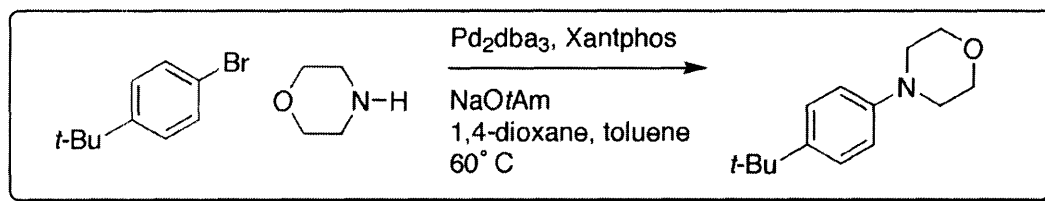


Figure 15 Fractional Conversion vs. Time for Calorimetric and GC Data. $[\text{ArBr}]_0 = 0.25\text{ M}$; $[\text{Amine}]_0 = 0.30\text{ M}$ (1.2 equivalents); $[\text{NaOtAm}]_0 = 0.35\text{ M}$ (1.4 equivalents); 1:1 Xantphos/Pd from $\text{Pd}_2(\text{dba})_3$ 2.5 mol % Pd based on ArBr; 1,4-Dioxane 3 ml, Toluene 1 ml.

Crystal Structure Determination of $\text{Pd}(t\text{-butylXantPhos})_2$. Crystals suitable for X-Ray diffraction were obtained by layering ether on a saturated solution of $\text{Pd}(t\text{-butylXantPhos})_2$ in benzene in a glovebox. A single crystal (0.17 x 0.12 x

0.09 mm³) was mounted on a magnetic glass pin and placed on the goniometer head under a stream of N₂ delivered from a Cyrostream 700 at 100K. A Siemens Platform three circle diffractometer equipped with an APEX CCD detector was used to obtain the data. The crystal was exposed to MoK_α radiation ($\lambda=0.71073$ Å), collecting 10 sec. frames, of which 230195 measured and 26495 independent reflections were observed, with $R_{int} = 0.1009$ in C2/c (space group #15), to $d=0.80$ ($2\theta=52.78^\circ$). Data was processed using SAINT supplied by Siemens Industrial Automation, Inc., and structure determination was completed by direct methods using SHELXTL, V6.10, G. M. Sheldrick, University of Göttingen. The structure was refined on F^2 by full-matrix least-squares methods, and absorption correction was applied with SADABS. All non-hydrogen atoms were refined anisotropically, except for the extremely disordered ether molecule. All hydrogens were placed in calculated positions and left to ride on their parent atoms. The benzene molecule was disordered and each carbon was set at half occupancy. The refinement of 1465 parameters using 26495 reflections and 0 restraints gave $R_1=0.0637$, $wR_2=0.1639$ [$I>2\sigma(I)$], goodness of fit on $F^2 = 1.070$, $\Delta\rho_{\max/\min} = 1.398/-0.967$ e.Å⁻³.

Magnetization Transfer Experiment. Pd(*t*-butylXantphos)₂ (34.2 mg, 0.0230 mmol) and *t*-butylXantphos (24.2 mg, 0.0350 mmol) were weighed inside of a glovebox into a small vial and dissolved in d₆-benzene (0.70 mL). This solution was placed inside of a screw-cap septum-sealed NMR tube. The tube was equilibrated in the NMR probe at either 20 °C or 60 °C. The free *t*-butylXantphos

was selectively inverted using a 180° pulse. After variable mixing times between 0.0100 and 5.12 s, a nonselective 90° pulse was applied. 16 transients with a relaxation delay of 35 s (T_1 of $\text{Pd}(t\text{-butylXantphos})_2$ is 1.17 s; T_1 of $t\text{-butylXantphos}$ is 6.46 s) was needed to obtain a spectrum with an acceptable signal to noise ratio. ^1H decoupling was applied during the 90° pulse. Integration values at the variable mixing times for the complex were determined.

Sample Analysis of Precatalyst by ^{31}P NMR. $t\text{-butylXantphos}$ (69.9 mg, 0.10 mmol) and $\text{Pd}_2(\text{dba})_3$ (45.9 mg, 0.0500 mmol) were dissolved in toluene (2.0 mL) and stirred for 2 h inside of a glovebox. This solution was filtered over a glass frit to remove insoluble matter, and concentrated to a volume of 0.7 mL. This solution was then transferred to a septum-sealed NMR tube.

Material Preparation

Preparation of $t\text{-butylXantphos}$. 4,5-dibromo-2,7-di-*tert*-butyl-9,9-dimethylxanthene (5.0 g, 10.4 mmol) was dissolved in THF (150 mL) in a 500 mL flame-dried round-bottom flask under argon. This solution was cooled to $-78\text{ }^\circ\text{C}$, and $n\text{-BuLi}$ (8.8 mL of a 2.5 M solution in hexanes, 22 mmol) was added dropwise over 20 min. The solution was stirred at $-78\text{ }^\circ\text{C}$ for 2 h, then chlorodiphenylphosphine (4.5 mL, 24 mmol) was added dropwise over 45 min. With stirring, the solution was allowed to warm to room temperature overnight. The solution was washed with water (3 X 100 ml), dried over MgSO_4 , and concentrated with the aid of a rotary evaporator to give a light yellow oil. With

vigorous stirring, EtOH (50 mL) was slowly added to the yellow oil to form a slurry of crude *t*-butylXantphos which was filtered and recrystallized from toluene/EtOH to afford 6.13 g (85%) of the white solid. ¹H NMR (CD₂Cl₂, 300 MHz): δ = 7.42 (d, ⁴J(H,H) = 2.40 Hz, 2H), 7.24 (m, 20H), 6.55 (m, 2H), 1.67 (s, 6H), 1.11 (s, 18H). ³¹P NMR{¹H} (CD₂Cl₂, 300 MHz): δ = -16.3; Lit. mp 194-195 °C,¹⁰ experimental mp 194-195 °C.

Preparation of PdCl₂(*t*-butylXantphos). Procedure was adapted from Hayashi's procedure to make PdCl₂(dppf).¹¹ A slurry of benzene (20 mL) and dichlorobis(acetonitrile)palladium (II) (518 mg, 2.00 mmol) was stirred in a septum-sealed 100 mL round-bottom flask in a glovebox under nitrogen atmosphere. *t*-butylXantphos (1.38 g, 2.00 mmol) was dissolved in benzene (20 mL) and added slowly with stirring to the dichlorobis(acetonitrile)palladium (II) slurry. This mixture was stirred for 12 hours during which time a yellow precipitate formed, as well as an orange solution. The yellow solid was filtered over a glass frit in a glovebox and washed with benzene (10 mL) and ether (10 mL) until the supernatant was clear, and finally dried under high vacuum to afford 457 mg (29%) of yellow solid. mp 171 °C dec; IR (KBr) 3057, 2964, 2906, 2869, 1479, 1436, 1426, 1395, 1364, 1255, 1234, 1190, 1094, 741, 706, 692 cm⁻¹; ¹H NMR (CD₂Cl₂, 300 MHz): δ = 7.70 (d, ⁴J(H,H) = 1.70 Hz, 2H), 7.23 (m, 22H), 1.87 (s, 6H), 1.26 (s, 18H); ¹³C NMR (CD₂Cl₂, 500 MHz): δ = 153.3 (m), 148.4 (m), 135.7 (m), 135.0 (m), 130.6 (s), 130.2 (s), 128.8 (s), 128.6 (s), 128.5 (s), 128.5 (s), 127.7 (s), 119.4 (m), 118.9 (m), 38.0 (m), 35.5 (s), 31.7 (s), 26.8 (bs)

(complexity of spectrum due to ^{31}P - ^{13}C coupling); ^{31}P NMR{ ^1H } (CD_2Cl_2 , 300 MHz): $\delta = 23.3$; MALDI-MS: Observed $\text{C}_{47}\text{H}_{48}\text{O}_2\text{P}_2\text{PdCl}$ (Complex-Cl): Theoretical 829.1907 (26.6%), 830.1922 (64.9%), 831.1915 (100.0%), 832.1927 (60.2%), 833.1907 (99.7%), 834.1935(45.4%), 835.1913 (57.5%), 836.1938 (25.7%), 837.1923 (14.9%); Found 829.2071 (35.8%), 830.2068 (76.1%), 831.2242 (100.0%), 832.1912 (70.5%), 833.2227 (97.3%), 834.2245 (51.2%), 835.1700 (59.4%), 836.2003 (25.6%), 837.1684 (5.5%).

Preparation of Cyclooctatetradienide Solution (0.30 M). As prepared previously by Katz and co-workers,¹² THF (16 mL) was added to a flame-dried 3-neck 25 mL round-bottom flask under argon and cooled to $-78\text{ }^\circ\text{C}$. Lithium granules (76 mg, 11 mmol, washed with hexanes to remove mineral oil) were added under a positive flow of argon. Cyclooctatetraene (0.54 mL, 4.8 mmol) was then added *via* syringe. The mixture was stirred overnight while warming to room temperature to form a green/blue solution that could be stirred at room temperature until use. Best results were obtained by using the solution the same day, but it can be stored for up to 4 days with minimal decomposition.

Preparation of Pd(*t*-butylXantphos)(cyclooctatetraene). Inside of a glovebox under nitrogen atmosphere, $\text{PdCl}_2(\textit{t}\text{-butylXantphos})$ (170 mg, 0.20 mmol) was weighed into a 25 mL round-bottom flask equipped with a stirbar. The flask was sealed with a rubber septum and further sealed with black electrical tape. The flask was removed from the glovebox and THF (8.0 mL) was

added to form a yellow slurry. The slurry was degassed by three freeze/pump/thaw cycles, and finally cooled to $-78\text{ }^{\circ}\text{C}$. Cyclooctatetraenide (0.70 mL of the 0.30 M solution in THF, 0.20 mmol) was added dropwise over five min and then stirred for thirty min to form a green slurry. Cannula transferring a portion of this solution to a flame-dried septum-sealed NMR tube under argon allowed for ^{31}P NMR analysis. Decomposition will begin to occur at room temperature, and this complex was not isolable. ^{31}P NMR $\{^1\text{H}\}$ (THF, 300 MHz): $\delta = 11.384$ (s).

Preparation of Pd(*t*-butylXantphos) $_2$. *t*-butylXantphos (830 mg, 1.2 mmol) was weighed into a 25 mL round-bottom flask and evacuated/backfilled with argon three times. The solid was dissolved in THF (5.0 mL), and then subjected to three freeze/pump/thaw cycles. While still cold, it was slowly cannula transferred to the Pd(*t*-butylXantphos)(cyclooctatetraene) solution prepared above. This mixture was stirred for thirty min while warming to rt to form a yellow solution. This yellow solution was taken into the glovebox and filtered. The resulting solution was concentrated, dissolved in benzene, filtered, and finally layered with ether. Bright yellow crystals formed which were suitable for X-Ray analysis (140 mg, 48 %). mp $162\text{ }^{\circ}\text{C}$ dec; IR (KBr) 3053, 2964, 2905, 2867, 2280, 1585, 1477, 1426, 1398, 1361, 1284, 1256, 1240, 742, 696 cm^{-1} ; ^1H NMR (C_6D_6 , 300 MHz): $\delta = 7.05$ (m, 48H), 1.78 (m, 12), 1.20 (m, 36H); ^{13}C NMR (C_6D_6 , 500 MHz): $\delta = 154.4$ (bs), 153.7 (bs), 145.3 (m), 141.7 (m), 139.7 (bs), 137.4 (bs), 135.0 (s), 133.9 (s), 132.7 (m), 131.2 (bs), 124.6 (m), 123.6 (m), 121.0 (m),

36.8 (s), 35.3, (m), 33.0 (s), 32.2 (m), 22.9 (bs); ^{31}P NMR{ ^1H } (C_6D_6 , 300 MHz): δ = 3.70 (m), 1.58 (m); Anal. Calcd. For $\text{C}_{94}\text{H}_{96}\text{O}_2\text{P}_4\text{Pd}$: C, 75.87; H, 6.50. Found: C, 75.97; H, 6.48.

Preparation of Pd(*t*-butylXantphos)(dba). Dibenzylideneacetone (280 mg, 1.2 mmol) was weighed into a 25 mL round-bottom flask and evacuated/backfilled with argon three times. The solid was dissolved in THF (5.0 mL), and was then subjected to three freeze/pump/thaw cycles. While still cold, it was slowly cannula transferred to the Pd(*t*-butylXantphos)(cyclooctatetraene) solution prepared above. This mixture was stirred for thirty min while warming to rt to form a red/yellow solution. All attempts to isolate this complex led to decomposition. However, ^{31}P NMR analysis prior to isolation attempts revealed the species previously observed in precatalyst solutions (see Figure 8). In solution before attempted isolation: ^{31}P NMR{ ^1H } (THF, 300 MHz): δ = 12.3 (d, $^2\text{J}(\text{P},\text{P}) = 29.1$ Hz), d = 9.82 (d, $^2\text{J}(\text{P},\text{P}) = 29.4$ Hz).

Preparation of Pd(Xantphos) $_2$. Xantphos (579 mg, 1.00 mmol) and $\text{Pd}_2(\text{dba})_3$ (229 mg, 0.250 mmol) were weighed into a flame-dried 500 mL round-bottom flask and evacuated/backfilled with argon three times. Toluene (300 mL) was added, and the solution was stirred for 4 h. The solution was then filtered with a cannula filter into another flame-dried round-bottom flask under argon to remove insoluble matter. This solution was concentrated slightly and allowed to rest overnight so that any extra palladium black would settle. The resulting solution

was filtered again, and finally concentrated to dryness. At this point, the yellow solid was stirred in toluene (100 mL) overnight to remove dibenzylidene acetone and excess Xantphos. The remaining yellow solid was isolated by filtration and is sparingly soluble in all common organic solvents. The identity of the species was confirmed to be Pd(Xantphos)₂ by use of MALDI-TOF-MS analysis and EA. IR (KBr) 2924, 2854, 1461, 1398, 1377, 1222 cm⁻¹; MALDI-MS: Anal. Calcd. For C₇₈H₆₄O₂P₄Pd: Theoretical 1260.2894 (22.9%), 1261.2909 (63.4%), 1262.2911 (100.0%), 1263.2907 (64.6%), 1264.2914 (77.2%), 1265.2933 (51.4%), 1266.2931 (43.7%), 1267.2949 (25.4%); Found 1260.3405 (24.0%), 1261.3285 (67.4%), 1262.3166 (100.0%), 1263.3162 (73.2%), 1264.3300 (79.3%), 1265.3424 (47.5%), 1266.3491 (35.5%), 1267.3104 (25.1%). Anal. Calcd. For C₇₈H₆₄O₂P₄Pd: C, 74.14; H, 5.10. Found: C, 74.44; H, 4.97; mp 164 °C dec.

Appendix A:

Selected Spectra:

STANDARD IN OBSERV

ppm x1000

SAMPLE 2085 0114 DEC. 8 VI
 DATE APR 15 2005 0114 208 101
 FOLVENT CDCl3 dn dn MS
 FT ACQUISITION exp dof 9
 SFRQ 100.101 dn dn min
 IN 11 dn dn C
 AT 1.995 dmf PRODUSSING 200
 NP 12084 vcl11c
 TD 101.000 PLOC not used
 B5 55 55 55
 Lpwr 55
 Pwr 7.0 wvr
 O1 1.000 wvr
 M0 15 wvr
 M1 15 wvr
 C1 15
 BLOC NOT USED
 GAIN 1
 I1 1
 I0 1
 DP 1
 DISKAY Y
 X0 16.1
 X1 272.3
 X2 272.3
 X3 272.3
 X4 272.3
 X5 272.3
 X6 272.3
 X7 272.3
 X8 272.3
 X9 272.3
 X10 272.3
 X11 272.3
 X12 272.3
 X13 272.3
 X14 272.3
 X15 272.3
 X16 272.3
 X17 272.3
 X18 272.3
 X19 272.3
 X20 272.3
 X21 272.3
 X22 272.3
 X23 272.3
 X24 272.3
 X25 272.3
 X26 272.3
 X27 272.3
 X28 272.3
 X29 272.3
 X30 272.3
 X31 272.3
 X32 272.3
 X33 272.3
 X34 272.3
 X35 272.3
 X36 272.3
 X37 272.3
 X38 272.3
 X39 272.3
 X40 272.3
 X41 272.3
 X42 272.3
 X43 272.3
 X44 272.3
 X45 272.3
 X46 272.3
 X47 272.3
 X48 272.3
 X49 272.3
 X50 272.3
 X51 272.3
 X52 272.3
 X53 272.3
 X54 272.3
 X55 272.3
 X56 272.3
 X57 272.3
 X58 272.3
 X59 272.3
 X60 272.3
 X61 272.3
 X62 272.3
 X63 272.3
 X64 272.3
 X65 272.3
 X66 272.3
 X67 272.3
 X68 272.3
 X69 272.3
 X70 272.3
 X71 272.3
 X72 272.3
 X73 272.3
 X74 272.3
 X75 272.3
 X76 272.3
 X77 272.3
 X78 272.3
 X79 272.3
 X80 272.3
 X81 272.3
 X82 272.3
 X83 272.3
 X84 272.3
 X85 272.3
 X86 272.3
 X87 272.3
 X88 272.3
 X89 272.3
 X90 272.3
 X91 272.3
 X92 272.3
 X93 272.3
 X94 272.3
 X95 272.3
 X96 272.3
 X97 272.3
 X98 272.3
 X99 272.3
 X100 272.3
 X101 272.3
 X102 272.3
 X103 272.3
 X104 272.3
 X105 272.3
 X106 272.3
 X107 272.3
 X108 272.3
 X109 272.3
 X110 272.3
 X111 272.3
 X112 272.3
 X113 272.3
 X114 272.3
 X115 272.3
 X116 272.3
 X117 272.3
 X118 272.3
 X119 272.3
 X120 272.3
 X121 272.3
 X122 272.3
 X123 272.3
 X124 272.3
 X125 272.3
 X126 272.3
 X127 272.3
 X128 272.3
 X129 272.3
 X130 272.3
 X131 272.3
 X132 272.3
 X133 272.3
 X134 272.3
 X135 272.3
 X136 272.3
 X137 272.3
 X138 272.3
 X139 272.3
 X140 272.3
 X141 272.3
 X142 272.3
 X143 272.3
 X144 272.3
 X145 272.3
 X146 272.3
 X147 272.3
 X148 272.3
 X149 272.3
 X150 272.3
 X151 272.3
 X152 272.3
 X153 272.3
 X154 272.3
 X155 272.3
 X156 272.3
 X157 272.3
 X158 272.3
 X159 272.3
 X160 272.3
 X161 272.3
 X162 272.3
 X163 272.3
 X164 272.3
 X165 272.3
 X166 272.3
 X167 272.3
 X168 272.3
 X169 272.3
 X170 272.3
 X171 272.3
 X172 272.3
 X173 272.3
 X174 272.3
 X175 272.3
 X176 272.3
 X177 272.3
 X178 272.3
 X179 272.3
 X180 272.3
 X181 272.3
 X182 272.3
 X183 272.3
 X184 272.3
 X185 272.3
 X186 272.3
 X187 272.3
 X188 272.3
 X189 272.3
 X190 272.3
 X191 272.3
 X192 272.3
 X193 272.3
 X194 272.3
 X195 272.3
 X196 272.3
 X197 272.3
 X198 272.3
 X199 272.3
 X200 272.3
 X201 272.3
 X202 272.3
 X203 272.3
 X204 272.3
 X205 272.3
 X206 272.3
 X207 272.3
 X208 272.3
 X209 272.3
 X210 272.3
 X211 272.3
 X212 272.3
 X213 272.3
 X214 272.3
 X215 272.3
 X216 272.3
 X217 272.3
 X218 272.3
 X219 272.3
 X220 272.3
 X221 272.3
 X222 272.3
 X223 272.3
 X224 272.3
 X225 272.3
 X226 272.3
 X227 272.3
 X228 272.3
 X229 272.3
 X230 272.3
 X231 272.3
 X232 272.3
 X233 272.3
 X234 272.3
 X235 272.3
 X236 272.3
 X237 272.3
 X238 272.3
 X239 272.3
 X240 272.3
 X241 272.3
 X242 272.3
 X243 272.3
 X244 272.3
 X245 272.3
 X246 272.3
 X247 272.3
 X248 272.3
 X249 272.3
 X250 272.3
 X251 272.3
 X252 272.3
 X253 272.3
 X254 272.3
 X255 272.3
 X256 272.3
 X257 272.3
 X258 272.3
 X259 272.3
 X260 272.3
 X261 272.3
 X262 272.3
 X263 272.3
 X264 272.3
 X265 272.3
 X266 272.3
 X267 272.3
 X268 272.3
 X269 272.3
 X270 272.3
 X271 272.3
 X272 272.3
 X273 272.3
 X274 272.3
 X275 272.3
 X276 272.3
 X277 272.3
 X278 272.3
 X279 272.3
 X280 272.3
 X281 272.3
 X282 272.3
 X283 272.3
 X284 272.3
 X285 272.3
 X286 272.3
 X287 272.3
 X288 272.3
 X289 272.3
 X290 272.3
 X291 272.3
 X292 272.3
 X293 272.3
 X294 272.3
 X295 272.3
 X296 272.3
 X297 272.3
 X298 272.3
 X299 272.3
 X300 272.3
 X301 272.3
 X302 272.3
 X303 272.3
 X304 272.3
 X305 272.3
 X306 272.3
 X307 272.3
 X308 272.3
 X309 272.3
 X310 272.3
 X311 272.3
 X312 272.3
 X313 272.3
 X314 272.3
 X315 272.3
 X316 272.3
 X317 272.3
 X318 272.3
 X319 272.3
 X320 272.3
 X321 272.3
 X322 272.3
 X323 272.3
 X324 272.3
 X325 272.3
 X326 272.3
 X327 272.3
 X328 272.3
 X329 272.3
 X330 272.3
 X331 272.3
 X332 272.3
 X333 272.3
 X334 272.3
 X335 272.3
 X336 272.3
 X337 272.3
 X338 272.3
 X339 272.3
 X340 272.3
 X341 272.3
 X342 272.3
 X343 272.3
 X344 272.3
 X345 272.3
 X346 272.3
 X347 272.3
 X348 272.3
 X349 272.3
 X350 272.3
 X351 272.3
 X352 272.3
 X353 272.3
 X354 272.3
 X355 272.3
 X356 272.3
 X357 272.3
 X358 272.3
 X359 272.3
 X360 272.3
 X361 272.3
 X362 272.3
 X363 272.3
 X364 272.3
 X365 272.3
 X366 272.3
 X367 272.3
 X368 272.3
 X369 272.3
 X370 272.3
 X371 272.3
 X372 272.3
 X373 272.3
 X374 272.3
 X375 272.3
 X376 272.3
 X377 272.3
 X378 272.3
 X379 272.3
 X380 272.3
 X381 272.3
 X382 272.3
 X383 272.3
 X384 272.3
 X385 272.3
 X386 272.3
 X387 272.3
 X388 272.3
 X389 272.3
 X390 272.3
 X391 272.3
 X392 272.3
 X393 272.3
 X394 272.3
 X395 272.3
 X396 272.3
 X397 272.3
 X398 272.3
 X399 272.3
 X400 272.3
 X401 272.3
 X402 272.3
 X403 272.3
 X404 272.3
 X405 272.3
 X406 272.3
 X407 272.3
 X408 272.3
 X409 272.3
 X410 272.3
 X411 272.3
 X412 272.3
 X413 272.3
 X414 272.3
 X415 272.3
 X416 272.3
 X417 272.3
 X418 272.3
 X419 272.3
 X420 272.3
 X421 272.3
 X422 272.3
 X423 272.3
 X424 272.3
 X425 272.3
 X426 272.3
 X427 272.3
 X428 272.3
 X429 272.3
 X430 272.3
 X431 272.3
 X432 272.3
 X433 272.3
 X434 272.3
 X435 272.3
 X436 272.3
 X437 272.3
 X438 272.3
 X439 272.3
 X440 272.3
 X441 272.3
 X442 272.3
 X443 272.3
 X444 272.3
 X445 272.3
 X446 272.3
 X447 272.3
 X448 272.3
 X449 272.3
 X450 272.3
 X451 272.3
 X452 272.3
 X453 272.3
 X454 272.3
 X455 272.3
 X456 272.3
 X457 272.3
 X458 272.3
 X459 272.3
 X460 272.3
 X461 272.3
 X462 272.3
 X463 272.3
 X464 272.3
 X465 272.3
 X466 272.3
 X467 272.3
 X468 272.3
 X469 272.3
 X470 272.3
 X471 272.3
 X472 272.3
 X473 272.3
 X474 272.3
 X475 272.3
 X476 272.3
 X477 272.3
 X478 272.3
 X479 272.3
 X480 272.3
 X481 272.3
 X482 272.3
 X483 272.3
 X484 272.3
 X485 272.3
 X486 272.3
 X487 272.3
 X488 272.3
 X489 272.3
 X490 272.3
 X491 272.3
 X492 272.3
 X493 272.3
 X494 272.3
 X495 272.3
 X496 272.3
 X497 272.3
 X498 272.3
 X499 272.3
 X500 272.3
 X501 272.3
 X502 272.3
 X503 272.3
 X504 272.3
 X505 272.3
 X506 272.3
 X507 272.3
 X508 272.3
 X509 272.3
 X510 272.3
 X511 272.3
 X512 272.3
 X513 272.3
 X514 272.3
 X515 272.3
 X516 272.3
 X517 272.3
 X518 272.3
 X519 272.3
 X520 272.3
 X521 272.3
 X522 272.3
 X523 272.3
 X524 272.3
 X525 272.3
 X526 272.3
 X527 272.3
 X528 272.3
 X529 272.3
 X530 272.3
 X531 272.3
 X532 272.3
 X533 272.3
 X534 272.3
 X535 272.3
 X536 272.3
 X537 272.3
 X538 272.3
 X539 272.3
 X540 272.3
 X541 272.3
 X542 272.3
 X543 272.3
 X544 272.3
 X545 272.3
 X546 272.3
 X547 272.3
 X548 272.3
 X549 272.3
 X550 272.3
 X551 272.3
 X552 272.3
 X553 272.3
 X554 272.3
 X555 272.3
 X556 272.3
 X557 272.3
 X558 272.3
 X559 272.3
 X560 272.3
 X561 272.3
 X562 272.3
 X563 272.3
 X564 272.3
 X565 272.3
 X566 272.3
 X567 272.3
 X568 272.3
 X569 272.3
 X570 272.3
 X571 272.3
 X572 272.3
 X573 272.3
 X574 272.3
 X575 272.3
 X576 272.3
 X577 272.3
 X578 272.3
 X579 272.3
 X580 272.3
 X581 272.3
 X582 272.3
 X583 272.3
 X584 272.3
 X585 272.3
 X586 272.3
 X587 272.3
 X588 272.3
 X589 272.3
 X590 272.3
 X591 272.3
 X592 272.3
 X593 272.3
 X594 272.3
 X595 272.3
 X596 272.3
 X597 272.3
 X598 272.3
 X599 272.3
 X600 272.3
 X601 272.3
 X602 272.3
 X603 272.3
 X604 272.3
 X605 272.3
 X606 272.3
 X607 272.3
 X608 272.3
 X609 272.3
 X610 272.3
 X611 272.3
 X612 272.3
 X613 272.3
 X614 272.3
 X615 272.3
 X616 272.3
 X617 272.3
 X618 272.3
 X619 272.3
 X620 272.3
 X621 272.3
 X622 272.3
 X623 272.3
 X624 272.3
 X625 272.3
 X626 272.3
 X627 272.3
 X628 272.3
 X629 272.3
 X630 272.3
 X631 272.3
 X632 272.3
 X633 272.3
 X634 272.3
 X635 272.3
 X636 272.3
 X637 272.3
 X638 272.3
 X639 272.3
 X640 272.3
 X641 272.3
 X642 272.3
 X643 272.3
 X644 272.3
 X645 272.3
 X646 272.3
 X647 272.3
 X648 272.3
 X649 272.3
 X650 272.3
 X651 272.3
 X652 272.3
 X653 272.3
 X654 272.3
 X655 272.3
 X656 272.3
 X657 272.3
 X658 272.3
 X659 272.3
 X660 272.3
 X661 272.3
 X662 272.3
 X663 272.3
 X664 272.3
 X665 272.3
 X666 272.3
 X667 272.3
 X668 272.3
 X669 272.3
 X670 272.3
 X671 272.3
 X672 272.3
 X673 272.3
 X674 272.3
 X675 272.3
 X676 272.3
 X677 272.3
 X678 272.3
 X679 272.3
 X680 272.3
 X681 272.3
 X682 272.3
 X683 272.3
 X684 272.3
 X685 272.3
 X686 272.3
 X687 272.3
 X688 272.3
 X689 272.3
 X690 272.3
 X691 272.3
 X692 272.3
 X693 272.3
 X694 272.3
 X695 272.3
 X696 272.3
 X697 272.3
 X698 272.3
 X699 272.3
 X700 272.3
 X701 272.3
 X702 272.3
 X703 272.3
 X704 272.3
 X705 272.3
 X706 272.3
 X707 272.3
 X708 272.3
 X709 272.3
 X710 272.3
 X711 272.3
 X712 272.3
 X713 272.3
 X714 272.3
 X715 272.3
 X716 272.3
 X717 272.3
 X718 272.3
 X719 272.3
 X720 272.3
 X721 272.3
 X722 272.3
 X723 272.3
 X724 272.3
 X725 272.3
 X726 272.3
 X727 272.3
 X728 272.3
 X729 272.3
 X730 272.3
 X731 272.3
 X732 272.3
 X733 272.3
 X734 272.3
 X735 272.3
 X736 272.3
 X737 272.3
 X738 272.3
 X739 272.3
 X740 272.3
 X741 272.3
 X742 272.3
 X743 272.3
 X744 272.3
 X745 272.3
 X746 272.3
 X747 272.3
 X748 272.3
 X749 272.3
 X750 272.3
 X751 272.3
 X752 272.3
 X753 272.3
 X754 272.3
 X755 272.3
 X756 272.3
 X757 272.3
 X758 272.3
 X759 272.3
 X760 272.3
 X761 272.3
 X762 272.3
 X763 272.3
 X764 272.3
 X765 272.3
 X766 272.3
 X767 272.3
 X768 272.3
 X769 272.3
 X770 272.3
 X771 272.3
 X772 272.3
 X773 272.3
 X774 272.3
 X775 272.3
 X776 272.3
 X777 272.3
 X778 272.3
 X779 272.3
 X780 272.3
 X781 272.3
 X782 272.3
 X783 272.3
 X784 272.3
 X785 272.3
 X786 272.3
 X787 272.3
 X788 272.3
 X789 272.3
 X790 272.3
 X791 272.3
 X792 272.3
 X793 272.3
 X794 272.3
 X795 272.3
 X796 272.3
 X797 272.3
 X798 272.3
 X799 272.3
 X800 272.3
 X801 272.3
 X802 272.3
 X803 272.3
 X804 272.3
 X805 272.3
 X806 272.3
 X807 272.3
 X808 272.3
 X809 272.3
 X810 272.3
 X811 272.3
 X812 272.3
 X813 272.3
 X814 272.3
 X815 272.3
 X816 272.3
 X817 272.3
 X818 272.3
 X819 272.3
 X820 272.3
 X821 272.3
 X822 272.3
 X823 272.3
 X824 272.3
 X825 272.3
 X826 272.3
 X827 272.3
 X828 272.3
 X829 272.3
 X830 272.3
 X831 272.3
 X832 272.3
 X833 272.3
 X834 272.3
 X835 272.3
 X836 272.3
 X837 272.3
 X838 272.3
 X839 272.3
 X840 272.3
 X841 272.3
 X842 272.3
 X843 272.3
 X844 272.3
 X845 272.3
 X846 272.3
 X847 272.3
 X848 272.3
 X849 272.3
 X850 272.3
 X851 272.3
 X852 272.3
 X853 272.3
 X854 272.3
 X855 272.3
 X856 272.3
 X857 272.3
 X858 272.3
 X859 272.3
 X860 272.3
 X861 272.3
 X862 272.3
 X863 272

X-Ray Crystallographic Data for Pd(Xantphos)₂

Table 1. Crystal data and structure refinement for 04168t.

Identification code	04168t	
Empirical formula	C ₁₆₂ H ₁₅₆ O ₄ P ₆ Pd ₂	
Formula weight	2563.78	
Temperature	100(2) K	
Wavelength	0.71073 Å	
Crystal system	Monoclinic	
Space group	C2/c	
Unit cell dimensions	a = 67.321(4) Å	α = 90°.
	b = 14.6266(8) Å	β = 112.7970(10)°.
	c = 28.5119(17) Å	γ = 90°.
Volume	25882(3) Å ³	
Z	4	
Density (calculated)	1.329 Mg/m ³	
Absorption coefficient	0.390 mm ⁻¹	
F(000)	10836	
Crystal size	0.17 x 0.12 x 0.09 mm ³	
Theta range for data collection	0.66 to 28.31°.	
Index ranges	-89 ≤ h ≤ 89, -19 ≤ k ≤ 19, -38 ≤ l ≤ 38	
Reflections collected	262953	
Independent reflections	32170 [R(int) = 0.1294]	
Completeness to theta = 28.31°	99.9 %	
Absorption correction	SADABS	
Refinement method	Full-matrix least-squares on F ²	
Data / restraints / parameters	32170 / 0 / 1397	
Goodness-of-fit on F ²	1.198	
Final R indices [I > 2σ(I)]	R1 = 0.0801, wR2 = 0.2530	
R indices (all data)	R1 = 0.1200, wR2 = 0.2911	
Largest diff. peak and hole	0.430 and -0.686 e.Å ⁻³	

Table 2. Atomic coordinates ($\times 10^4$) and equivalent isotropic displacement parameters ($\text{\AA}^2 \times 10^3$) for 04168t. $U(\text{eq})$ is defined as one third of the trace of the orthogonalized U^{ij} tensor.

	x	y	z	$U(\text{eq})$
C(140)	1610(3)	4746(15)	4082(4)	255(12)
C(1)	973(1)	921(7)	385(3)	77(3)
Pd(1)	0	7664(1)	2500	27(1)
P(7)	65(1)	8520(1)	1862(1)	28(1)
P(8)	306(1)	6723(1)	2934(1)	33(1)
O(3)	357(1)	6966(3)	1988(1)	33(1)
C(3)	306(1)	9253(3)	2068(2)	30(1)
C(4)	302(1)	6101(4)	3498(2)	41(1)
C(5)	-140(1)	9360(4)	1482(2)	32(1)
C(6)	247(1)	7141(4)	1474(2)	34(1)
C(7)	357(1)	5788(4)	2560(2)	36(1)
C(8)	404(1)	4202(4)	2350(2)	40(1)
C(9)	-352(1)	9037(5)	1232(2)	43(1)
C(10)	283(1)	6592(4)	1113(2)	37(1)
C(11)	636(1)	9822(4)	2015(2)	41(1)
C(12)	341(1)	9830(4)	2486(2)	32(1)
C(13)	447(1)	5815(4)	1321(2)	41(1)
C(14)	668(1)	10403(4)	2431(2)	40(1)
C(15)	416(1)	5421(4)	1782(2)	36(1)
C(16)	106(1)	7876(4)	1344(2)	34(1)
C(17)	0(1)	8102(4)	817(2)	38(1)
C(18)	456(1)	9245(4)	1839(2)	37(1)
C(19)	377(1)	6048(4)	2107(2)	34(1)
C(20)	374(1)	4862(4)	2683(2)	39(1)
C(21)	584(1)	7172(4)	3186(2)	37(1)
C(22)	174(1)	6815(4)	600(2)	41(1)
C(23)	521(1)	10392(4)	2661(2)	35(1)
C(24)	-94(1)	10291(4)	1455(2)	42(1)
C(25)	36(1)	7560(4)	448(2)	43(1)
C(26)	-516(1)	9624(5)	960(3)	53(2)
C(27)	680(1)	6214(5)	1511(3)	49(2)

C(28)	-476(1)	10561(5)	928(3)	54(2)
C(29)	623(1)	8097(5)	3169(2)	45(1)
C(30)	-84(1)	7830(5)	-118(2)	46(2)
C(31)	427(1)	4494(4)	1911(2)	41(1)
C(32)	833(1)	8447(5)	3352(2)	53(2)
C(33)	145(1)	5427(5)	3427(3)	49(2)
C(34)	-262(1)	10904(5)	1189(3)	56(2)
C(35)	427(1)	3182(4)	2497(2)	43(1)
C(36)	129(1)	4970(5)	3851(3)	55(2)
C(37)	1006(1)	7876(6)	3562(2)	59(2)
C(38)	440(1)	6347(5)	3990(2)	58(2)
C(39)	424(1)	5079(4)	911(3)	53(2)
C(40)	419(2)	5910(6)	4403(3)	70(2)
C(41)	272(1)	5227(5)	4343(3)	58(2)
C(42)	762(1)	6576(5)	3401(3)	68(2)
C(43)	665(1)	2932(5)	2681(3)	64(2)
C(44)	-6(2)	7206(6)	-472(3)	74(2)
C(45)	-25(2)	8813(6)	-189(3)	78(3)
C(46)	-318(1)	7639(9)	-265(3)	96(4)
C(47)	295(1)	2596(5)	2045(3)	72(2)
C(48)	969(1)	6923(6)	3589(3)	74(3)
C(49)	351(2)	2978(6)	2936(4)	97(4)
Pd(2)	1838(1)	731(1)	2765(1)	25(1)
P(3)	2097(1)	-416(1)	3190(1)	28(1)
P(4)	1792(1)	958(1)	1901(1)	26(1)
P(5)	1499(1)	296(1)	2777(1)	27(1)
P(6)	1945(1)	2145(1)	3222(1)	28(1)
O(2)	1737(1)	2834(3)	2192(1)	31(1)
O(1)	1773(1)	-727(3)	3639(1)	32(1)
C(52)	1472(1)	265(4)	3400(2)	28(1)
C(53)	1576(1)	2626(4)	1726(2)	29(1)
C(54)	1711(1)	-55(4)	1481(2)	31(1)
C(55)	2051(1)	-1593(4)	2930(2)	30(1)
C(56)	2151(1)	-660(4)	3865(2)	32(1)
C(57)	1174(1)	1331(4)	4177(2)	36(1)
C(58)	1417(1)	3290(4)	1486(2)	35(1)

C(59)	2221(1)	905(4)	2003(2)	31(1)
C(60)	1378(1)	-844(4)	2563(2)	28(1)
C(61)	1327(1)	720(4)	4030(2)	32(1)
C(62)	1978(1)	-757(4)	4016(2)	34(1)
C(63)	2299(1)	2396(4)	2956(2)	31(1)
C(64)	1178(1)	-1083(4)	2572(2)	35(1)
C(65)	1320(1)	742(4)	3531(2)	30(1)
C(66)	2376(1)	-207(4)	3249(2)	31(1)
C(67)	2184(1)	2752(4)	3226(2)	29(1)
C(68)	1253(1)	2198(5)	797(2)	46(2)
C(69)	1114(1)	803(4)	1934(2)	38(1)
C(70)	2002(1)	2063(4)	3905(2)	32(1)
C(71)	2023(1)	1355(4)	1757(2)	29(1)
C(72)	2037(1)	-2351(4)	3209(2)	34(1)
C(73)	2490(1)	-767(4)	3035(2)	37(1)
C(74)	1422(1)	1578(4)	1041(2)	36(1)
C(75)	2023(1)	-1710(4)	2421(2)	34(1)
C(76)	1672(1)	3369(4)	2513(2)	35(1)
C(77)	2012(1)	2080(4)	1422(2)	33(1)
C(78)	1482(1)	161(4)	4395(2)	35(1)
C(79)	2699(1)	-519(4)	3089(2)	41(1)
C(80)	1584(1)	1775(4)	1527(2)	31(1)
C(81)	1760(1)	3150(4)	3028(2)	35(1)
C(82)	1624(1)	-250(4)	3776(2)	30(1)
C(83)	2360(1)	-733(4)	4243(2)	35(1)
C(84)	2213(1)	2034(4)	4269(2)	36(1)
C(85)	1088(1)	-1937(4)	2405(2)	40(1)
C(86)	1523(1)	-511(4)	1441(2)	41(1)
C(87)	2393(1)	-836(4)	4751(2)	36(1)
C(88)	2442(1)	4005(4)	3510(3)	46(1)
C(89)	2477(1)	585(4)	3515(2)	41(1)
C(90)	1276(1)	1066(4)	2405(2)	29(1)
C(91)	2403(1)	1159(4)	1915(2)	34(1)
C(92)	1989(1)	-2589(4)	2201(2)	41(1)
C(93)	1490(1)	-1491(4)	2406(2)	35(1)
C(94)	2194(1)	2333(4)	1340(2)	39(1)

C(95)	1632(1)	-337(4)	4271(2)	36(1)
C(96)	2214(1)	-894(4)	4891(2)	41(1)
C(97)	1119(1)	2603(5)	2288(3)	45(2)
C(98)	2689(1)	817(5)	3582(2)	46(1)
C(99)	1837(1)	-429(4)	1232(2)	39(1)
C(100)	2627(1)	-845(5)	5154(2)	43(1)
C(101)	1436(1)	4226(4)	1732(2)	41(1)
C(102)	2258(1)	3579(4)	3505(2)	40(1)
C(103)	1799(1)	-983(4)	4634(2)	40(1)
C(104)	2087(1)	1773(5)	4947(2)	51(2)
C(105)	1466(1)	4605(5)	2644(3)	48(2)
C(106)	2004(1)	-859(4)	4521(2)	38(1)
C(107)	1834(1)	1937(5)	4070(2)	48(2)
C(108)	1279(1)	1966(4)	2572(2)	36(1)
C(109)	1703(1)	3708(5)	3357(2)	42(1)
C(110)	2559(1)	3622(4)	3234(2)	41(1)
C(111)	1524(1)	4068(4)	2309(2)	40(1)
C(112)	2390(1)	1881(4)	1586(2)	38(1)
C(113)	2001(1)	-3229(4)	2995(2)	42(1)
C(114)	2256(1)	1879(5)	4790(2)	44(1)
C(115)	1983(1)	-3349(4)	2488(2)	41(1)
C(116)	1843(1)	-758(6)	5191(2)	61(2)
C(117)	1776(1)	-1259(5)	965(2)	47(2)
C(118)	2484(1)	2830(4)	2956(2)	36(1)
C(119)	1720(1)	-1979(5)	4505(3)	52(2)
C(120)	1403(1)	-2351(4)	2236(3)	45(1)
C(121)	1606(1)	4786(5)	1600(3)	54(2)
C(122)	1873(1)	1818(6)	4585(2)	58(2)
C(123)	1254(1)	3044(5)	1017(2)	41(1)
C(124)	1556(1)	4410(5)	3173(3)	51(2)
C(125)	957(1)	1427(5)	1651(2)	44(1)
C(126)	955(1)	2329(5)	1822(3)	50(2)
C(127)	1071(1)	1891(7)	287(2)	70(2)
C(128)	1486(1)	4988(6)	3538(3)	65(2)
C(129)	1589(1)	-1718(5)	933(2)	53(2)
C(130)	1260(2)	4699(7)	3470(6)	139(6)

C(131)	1457(1)	-1330(5)	1161(2)	53(2)
C(132)	2699(1)	168(6)	5272(3)	66(2)
C(133)	2782(1)	-1323(7)	4964(3)	82(3)
C(134)	1484(3)	6000(7)	3417(6)	151(7)
C(135)	1157(1)	1631(8)	-94(3)	83(3)
C(137)	2638(1)	-1289(7)	5660(3)	79(3)
C(138)	1255(3)	2302(8)	4223(9)	246(12)
C(139)	950(1)	1331(9)	3769(3)	110(4)
C(141)	1200(1)	-2578(4)	2231(3)	46(1)
C(142)	2800(1)	264(4)	3365(2)	43(1)
C(143)	1223(1)	4762(5)	1540(3)	52(2)
C(144)	879(1)	2458(8)	157(4)	96(3)
C(145)	1157(2)	1015(11)	4665(4)	161(7)
C(200)	1564(2)	3974(8)	296(4)	108(3)
C(201)	1379(2)	4540(8)	105(4)	109(3)
C(207)	1790(2)	4832(8)	5407(4)	111(3)
C(206)	1628(2)	4156(9)	5241(5)	145(4)
C(202)	736(2)	7524(10)	285(6)	157(5)
C(205)	1405(2)	4520(10)	5073(5)	144(4)
C(204)	735(3)	8784(12)	886(6)	196(5)
C(203)	784(3)	8194(13)	573(7)	206(6)

Table 3. Bond lengths [Å] and angles [°] for 04168t.

C(140)-C(128)	1.492(14)
C(1)-C(127)	1.636(13)
Pd(1)-P(7)	2.3844(13)
Pd(1)-P(7)#1	2.3844(13)
Pd(1)-P(8)#1	2.3878(14)
Pd(1)-P(8)	2.3878(14)
P(7)-C(5)	1.851(5)
P(7)-C(3)	1.838(5)
P(7)-C(16)	1.860(5)
P(8)-C(7)	1.844(5)
P(8)-C(21)	1.842(6)
P(8)-C(4)	1.859(6)
O(3)-C(6)	1.387(6)
O(3)-C(19)	1.379(7)
C(3)-C(12)	1.402(7)
C(3)-C(18)	1.403(7)
C(4)-C(33)	1.398(9)
C(4)-C(38)	1.397(8)
C(5)-C(24)	1.404(8)
C(5)-C(9)	1.406(8)
C(6)-C(16)	1.387(8)
C(6)-C(10)	1.398(7)
C(7)-C(20)	1.394(8)
C(7)-C(19)	1.404(8)
C(8)-C(31)	1.387(8)
C(8)-C(20)	1.423(8)
C(8)-C(35)	1.541(8)
C(9)-C(26)	1.378(9)
C(10)-C(22)	1.397(8)
C(10)-C(13)	1.532(9)
C(11)-C(18)	1.401(8)
C(11)-C(14)	1.407(8)
C(12)-C(23)	1.383(7)
C(13)-C(15)	1.519(8)

C(13)-C(39)	1.553(8)
C(13)-C(27)	1.563(8)
C(14)-C(23)	1.387(8)
C(15)-C(31)	1.400(8)
C(15)-C(19)	1.399(7)
C(16)-C(17)	1.431(7)
C(17)-C(25)	1.412(8)
C(21)-C(29)	1.384(9)
C(21)-C(42)	1.418(8)
C(22)-C(25)	1.389(9)
C(24)-C(34)	1.412(9)
C(25)-C(30)	1.548(8)
C(26)-C(28)	1.407(10)
C(28)-C(34)	1.430(10)
C(29)-C(32)	1.399(9)
C(30)-C(46)	1.491(10)
C(30)-C(45)	1.527(10)
C(30)-C(44)	1.592(10)
C(32)-C(37)	1.371(10)
C(33)-C(36)	1.423(9)
C(35)-C(47)	1.517(9)
C(35)-C(49)	1.553(10)
C(35)-C(43)	1.523(9)
C(36)-C(41)	1.410(10)
C(37)-C(48)	1.423(12)
C(38)-C(40)	1.395(10)
C(40)-C(41)	1.370(12)
C(42)-C(48)	1.383(11)
Pd(2)-P(5)	2.3809(13)
Pd(2)-P(4)	2.3857(12)
Pd(2)-P(3)	2.3846(14)
Pd(2)-P(6)	2.4001(14)
P(3)-C(66)	1.847(5)
P(3)-C(56)	1.849(5)
P(3)-C(55)	1.852(6)
P(4)-C(80)	1.835(5)

P(4)-C(54)	1.848(5)
P(4)-C(71)	1.850(5)
P(5)-C(60)	1.853(5)
P(5)-C(90)	1.845(5)
P(5)-C(52)	1.855(5)
P(6)-C(70)	1.837(5)
P(6)-C(67)	1.836(5)
P(6)-C(81)	1.866(6)
O(2)-C(53)	1.383(6)
O(2)-C(76)	1.395(6)
O(1)-C(62)	1.381(6)
O(1)-C(82)	1.397(6)
C(52)-C(82)	1.383(7)
C(52)-C(65)	1.402(7)
C(53)-C(80)	1.377(7)
C(53)-C(58)	1.411(7)
C(54)-C(86)	1.392(8)
C(54)-C(99)	1.412(7)
C(55)-C(72)	1.388(8)
C(55)-C(75)	1.400(6)
C(56)-C(83)	1.409(7)
C(56)-C(62)	1.396(7)
C(57)-C(138)	1.507(12)
C(57)-C(139)	1.507(9)
C(57)-C(61)	1.538(7)
C(57)-C(145)	1.512(10)
C(58)-C(123)	1.408(8)
C(58)-C(101)	1.522(8)
C(59)-C(91)	1.390(7)
C(59)-C(71)	1.409(7)
C(60)-C(64)	1.395(7)
C(60)-C(93)	1.391(7)
C(61)-C(65)	1.407(7)
C(61)-C(78)	1.413(7)
C(62)-C(106)	1.388(7)
C(63)-C(67)	1.386(7)

C(63)-C(118)	1.396(7)
C(64)-C(85)	1.390(8)
C(66)-C(89)	1.407(8)
C(66)-C(73)	1.414(7)
C(67)-C(102)	1.427(8)
C(68)-C(74)	1.409(8)
C(68)-C(123)	1.386(9)
C(68)-C(127)	1.560(9)
C(69)-C(125)	1.394(8)
C(69)-C(90)	1.417(7)
C(70)-C(84)	1.394(7)
C(70)-C(107)	1.398(7)
C(71)-C(77)	1.408(7)
C(72)-C(113)	1.403(8)
C(73)-C(79)	1.400(7)
C(74)-C(80)	1.423(7)
C(75)-C(92)	1.412(8)
C(76)-C(111)	1.388(8)
C(76)-C(81)	1.392(7)
C(77)-C(94)	1.385(7)
C(78)-C(95)	1.397(7)
C(79)-C(142)	1.406(9)
C(81)-C(109)	1.403(7)
C(82)-C(95)	1.397(7)
C(83)-C(87)	1.384(7)
C(84)-C(114)	1.418(7)
C(85)-C(141)	1.411(8)
C(86)-C(131)	1.413(9)
C(87)-C(96)	1.411(8)
C(87)-C(100)	1.547(8)
C(88)-C(102)	1.381(8)
C(88)-C(110)	1.425(8)
C(89)-C(98)	1.401(8)
C(90)-C(108)	1.398(8)
C(91)-C(112)	1.392(8)
C(92)-C(115)	1.390(9)

C(93)-C(120)	1.394(8)
C(94)-C(112)	1.399(8)
C(95)-C(103)	1.525(7)
C(96)-C(106)	1.401(8)
C(97)-C(108)	1.417(8)
C(97)-C(126)	1.416(9)
C(98)-C(142)	1.402(9)
C(99)-C(117)	1.407(8)
C(100)-C(133)	1.520(9)
C(100)-C(132)	1.556(10)
C(100)-C(137)	1.559(9)
C(101)-C(111)	1.536(8)
C(101)-C(143)	1.538(8)
C(101)-C(121)	1.565(9)
C(103)-C(116)	1.534(8)
C(103)-C(106)	1.544(8)
C(103)-C(119)	1.545(10)
C(104)-C(114)	1.380(8)
C(104)-C(122)	1.414(9)
C(105)-C(124)	1.419(9)
C(105)-C(111)	1.403(8)
C(107)-C(122)	1.400(8)
C(109)-C(124)	1.382(9)
C(110)-C(118)	1.384(8)
C(113)-C(115)	1.413(8)
C(117)-C(129)	1.394(9)
C(120)-C(141)	1.398(8)
C(124)-C(128)	1.548(9)
C(125)-C(126)	1.407(10)
C(127)-C(144)	1.458(11)
C(127)-C(135)	1.465(10)
C(128)-C(130)	1.517(13)
C(128)-C(134)	1.519(14)
C(129)-C(131)	1.413(10)
C(200)-C(201)	1.419(15)
C(201)-C(205)#2	1.394(16)

C(207)-C(206)	1.413(16)
C(206)-C(205)	1.487(17)
C(202)-C(203)	1.239(19)
C(205)-C(201)#3	1.394(16)
C(204)-C(203)	1.37(2)
P(7)-Pd(1)-P(7)#1	116.68(7)
P(7)-Pd(1)-P(8)#1	106.51(4)
P(7)#1-Pd(1)-P(8)#1	108.73(5)
P(7)-Pd(1)-P(8)	108.73(5)
P(7)#1-Pd(1)-P(8)	106.51(4)
P(8)#1-Pd(1)-P(8)	109.58(8)
C(5)-P(7)-C(3)	99.4(2)
C(5)-P(7)-C(16)	100.2(2)
C(3)-P(7)-C(16)	99.6(2)
C(5)-P(7)-Pd(1)	118.71(16)
C(3)-P(7)-Pd(1)	117.44(17)
C(16)-P(7)-Pd(1)	117.87(18)
C(7)-P(8)-C(21)	96.0(2)
C(7)-P(8)-C(4)	101.9(3)
C(21)-P(8)-C(4)	101.0(3)
C(7)-P(8)-Pd(1)	116.30(18)
C(21)-P(8)-Pd(1)	122.5(2)
C(4)-P(8)-Pd(1)	115.46(18)
C(6)-O(3)-C(19)	113.6(4)
C(12)-C(3)-C(18)	118.9(5)
C(12)-C(3)-P(7)	117.6(4)
C(18)-C(3)-P(7)	123.4(4)
C(33)-C(4)-C(38)	119.9(6)
C(33)-C(4)-P(8)	118.9(5)
C(38)-C(4)-P(8)	121.0(5)
C(24)-C(5)-C(9)	119.8(5)
C(24)-C(5)-P(7)	123.2(4)
C(9)-C(5)-P(7)	116.9(4)
C(16)-C(6)-O(3)	117.0(4)
C(16)-C(6)-C(10)	123.0(5)

O(3)-C(6)-C(10)	120.0(5)
C(20)-C(7)-C(19)	117.9(5)
C(20)-C(7)-P(8)	126.2(4)
C(19)-C(7)-P(8)	115.9(4)
C(31)-C(8)-C(20)	119.3(5)
C(31)-C(8)-C(35)	120.5(5)
C(20)-C(8)-C(35)	120.0(5)
C(26)-C(9)-C(5)	120.8(6)
C(22)-C(10)-C(6)	117.8(6)
C(22)-C(10)-C(13)	125.9(5)
C(6)-C(10)-C(13)	116.2(5)
C(18)-C(11)-C(14)	119.7(5)
C(23)-C(12)-C(3)	120.1(5)
C(10)-C(13)-C(15)	107.5(4)
C(10)-C(13)-C(39)	112.0(5)
C(15)-C(13)-C(39)	112.5(5)
C(10)-C(13)-C(27)	109.4(5)
C(15)-C(13)-C(27)	107.2(5)
C(39)-C(13)-C(27)	108.1(5)
C(23)-C(14)-C(11)	119.1(5)
C(31)-C(15)-C(19)	117.7(5)
C(31)-C(15)-C(13)	125.8(5)
C(19)-C(15)-C(13)	116.6(5)
C(6)-C(16)-C(17)	118.1(5)
C(6)-C(16)-P(7)	118.6(4)
C(17)-C(16)-P(7)	123.3(4)
C(25)-C(17)-C(16)	119.5(6)
C(3)-C(18)-C(11)	120.6(5)
O(3)-C(19)-C(15)	120.1(5)
O(3)-C(19)-C(7)	117.1(4)
C(15)-C(19)-C(7)	122.9(5)
C(7)-C(20)-C(8)	120.6(5)
C(29)-C(21)-C(42)	118.3(6)
C(29)-C(21)-P(8)	121.0(4)
C(42)-C(21)-P(8)	120.7(5)
C(25)-C(22)-C(10)	121.8(5)

C(14)-C(23)-C(12)	121.5(5)
C(5)-C(24)-C(34)	120.0(6)
C(22)-C(25)-C(17)	119.8(5)
C(22)-C(25)-C(30)	122.8(5)
C(17)-C(25)-C(30)	117.5(6)
C(28)-C(26)-C(9)	120.7(6)
C(26)-C(28)-C(34)	119.2(6)
C(21)-C(29)-C(32)	121.7(6)
C(46)-C(30)-C(25)	108.2(5)
C(46)-C(30)-C(45)	116.1(8)
C(25)-C(30)-C(45)	108.8(5)
C(46)-C(30)-C(44)	106.5(7)
C(25)-C(30)-C(44)	110.3(6)
C(45)-C(30)-C(44)	106.8(6)
C(8)-C(31)-C(15)	121.6(5)
C(37)-C(32)-C(29)	120.4(7)
C(4)-C(33)-C(36)	120.6(6)
C(24)-C(34)-C(28)	119.4(6)
C(47)-C(35)-C(49)	108.0(7)
C(47)-C(35)-C(43)	110.5(6)
C(49)-C(35)-C(43)	107.9(7)
C(47)-C(35)-C(8)	110.6(6)
C(49)-C(35)-C(8)	111.9(5)
C(43)-C(35)-C(8)	108.0(5)
C(41)-C(36)-C(33)	118.2(7)
C(32)-C(37)-C(48)	118.9(7)
C(40)-C(38)-C(4)	118.9(7)
C(41)-C(40)-C(38)	122.2(7)
C(40)-C(41)-C(36)	120.0(6)
C(21)-C(42)-C(48)	120.0(8)
C(37)-C(48)-C(42)	120.7(7)
P(5)-Pd(2)-P(4)	108.07(4)
P(5)-Pd(2)-P(3)	108.73(5)
P(4)-Pd(2)-P(3)	113.51(4)
P(5)-Pd(2)-P(6)	108.09(4)
P(4)-Pd(2)-P(6)	109.40(5)

P(3)-Pd(2)-P(6)	108.90(5)
C(66)-P(3)-C(56)	98.9(2)
C(66)-P(3)-C(55)	101.3(2)
C(56)-P(3)-C(55)	99.9(2)
C(66)-P(3)-Pd(2)	116.64(18)
C(56)-P(3)-Pd(2)	118.29(17)
C(55)-P(3)-Pd(2)	118.38(16)
C(80)-P(4)-C(54)	100.3(2)
C(80)-P(4)-C(71)	100.6(2)
C(54)-P(4)-C(71)	99.9(2)
C(80)-P(4)-Pd(2)	117.05(16)
C(54)-P(4)-Pd(2)	116.40(17)
C(71)-P(4)-Pd(2)	119.31(16)
C(60)-P(5)-C(90)	101.8(2)
C(60)-P(5)-C(52)	95.7(2)
C(90)-P(5)-C(52)	101.9(2)
C(60)-P(5)-Pd(2)	122.55(16)
C(90)-P(5)-Pd(2)	113.44(16)
C(52)-P(5)-Pd(2)	117.99(16)
C(70)-P(6)-C(67)	101.5(2)
C(70)-P(6)-C(81)	102.0(2)
C(67)-P(6)-C(81)	95.9(2)
C(70)-P(6)-Pd(2)	114.54(18)
C(67)-P(6)-Pd(2)	119.90(17)
C(81)-P(6)-Pd(2)	119.56(17)
C(53)-O(2)-C(76)	115.3(4)
C(62)-O(1)-C(82)	113.9(4)
C(82)-C(52)-C(65)	117.5(4)
C(82)-C(52)-P(5)	115.9(4)
C(65)-C(52)-P(5)	126.5(4)
C(80)-C(53)-O(2)	117.0(4)
C(80)-C(53)-C(58)	124.3(5)
O(2)-C(53)-C(58)	118.6(5)
C(86)-C(54)-C(99)	118.3(5)
C(86)-C(54)-P(4)	118.0(4)
C(99)-C(54)-P(4)	123.5(4)

C(72)-C(55)-C(75)	119.0(5)
C(72)-C(55)-P(3)	123.4(4)
C(75)-C(55)-P(3)	117.5(4)
C(83)-C(56)-C(62)	117.5(5)
C(83)-C(56)-P(3)	123.1(4)
C(62)-C(56)-P(3)	119.3(4)
C(138)-C(57)-C(139)	106.7(11)
C(138)-C(57)-C(61)	108.3(5)
C(139)-C(57)-C(61)	111.4(5)
C(138)-C(57)-C(145)	111.3(11)
C(139)-C(57)-C(145)	107.4(8)
C(61)-C(57)-C(145)	111.8(5)
C(123)-C(58)-C(53)	116.8(5)
C(123)-C(58)-C(101)	124.3(5)
C(53)-C(58)-C(101)	118.8(5)
C(91)-C(59)-C(71)	121.0(5)
C(64)-C(60)-C(93)	118.9(5)
C(64)-C(60)-P(5)	121.5(4)
C(93)-C(60)-P(5)	119.5(4)
C(65)-C(61)-C(78)	118.8(4)
C(65)-C(61)-C(57)	120.0(5)
C(78)-C(61)-C(57)	121.2(4)
C(106)-C(62)-O(1)	119.9(5)
C(106)-C(62)-C(56)	123.0(5)
O(1)-C(62)-C(56)	117.1(4)
C(67)-C(63)-C(118)	121.1(5)
C(85)-C(64)-C(60)	121.1(5)
C(52)-C(65)-C(61)	121.1(5)
C(89)-C(66)-C(73)	118.6(5)
C(89)-C(66)-P(3)	116.7(4)
C(73)-C(66)-P(3)	124.7(4)
C(63)-C(67)-C(102)	118.6(5)
C(63)-C(67)-P(6)	119.4(4)
C(102)-C(67)-P(6)	122.0(4)
C(74)-C(68)-C(123)	119.3(5)
C(74)-C(68)-C(127)	117.7(6)

C(123)-C(68)-C(127)	122.9(6)
C(125)-C(69)-C(90)	120.3(6)
C(84)-C(70)-C(107)	118.0(5)
C(84)-C(70)-P(6)	121.8(4)
C(107)-C(70)-P(6)	119.9(4)
C(77)-C(71)-C(59)	118.8(5)
C(77)-C(71)-P(4)	123.9(4)
C(59)-C(71)-P(4)	117.4(4)
C(55)-C(72)-C(113)	121.3(5)
C(79)-C(73)-C(66)	119.5(5)
C(68)-C(74)-C(80)	121.1(5)
C(55)-C(75)-C(92)	120.4(5)
C(111)-C(76)-C(81)	123.6(5)
C(111)-C(76)-O(2)	119.6(5)
C(81)-C(76)-O(2)	116.8(5)
C(94)-C(77)-C(71)	119.8(5)
C(95)-C(78)-C(61)	121.1(5)
C(73)-C(79)-C(142)	121.3(5)
C(53)-C(80)-C(74)	116.7(5)
C(53)-C(80)-P(4)	119.4(4)
C(74)-C(80)-P(4)	123.9(4)
C(76)-C(81)-C(109)	117.1(5)
C(76)-C(81)-P(6)	117.1(4)
C(109)-C(81)-P(6)	125.8(4)
C(52)-C(82)-C(95)	124.0(5)
C(52)-C(82)-O(1)	116.9(4)
C(95)-C(82)-O(1)	119.1(4)
C(56)-C(83)-C(87)	121.2(5)
C(70)-C(84)-C(114)	121.4(5)
C(64)-C(85)-C(141)	119.5(5)
C(131)-C(86)-C(54)	122.2(6)
C(96)-C(87)-C(83)	119.4(5)
C(96)-C(87)-C(100)	121.5(5)
C(83)-C(87)-C(100)	119.0(5)
C(102)-C(88)-C(110)	120.1(5)
C(98)-C(89)-C(66)	121.8(6)

C(108)-C(90)-C(69)	118.7(5)
C(108)-C(90)-P(5)	118.7(4)
C(69)-C(90)-P(5)	122.4(4)
C(59)-C(91)-C(112)	119.7(5)
C(115)-C(92)-C(75)	120.3(5)
C(120)-C(93)-C(60)	121.0(5)
C(77)-C(94)-C(112)	121.0(5)
C(82)-C(95)-C(78)	117.3(5)
C(82)-C(95)-C(103)	118.1(5)
C(78)-C(95)-C(103)	124.5(5)
C(87)-C(96)-C(106)	120.6(5)
C(108)-C(97)-C(126)	119.5(6)
C(89)-C(98)-C(142)	119.3(6)
C(117)-C(99)-C(54)	120.0(6)
C(133)-C(100)-C(132)	108.3(7)
C(133)-C(100)-C(137)	110.3(6)
C(132)-C(100)-C(137)	107.3(6)
C(133)-C(100)-C(87)	112.3(5)
C(132)-C(100)-C(87)	107.2(5)
C(137)-C(100)-C(87)	111.2(5)
C(111)-C(101)-C(58)	106.7(5)
C(111)-C(101)-C(143)	112.1(5)
C(58)-C(101)-C(143)	113.2(5)
C(111)-C(101)-C(121)	108.9(5)
C(58)-C(101)-C(121)	107.5(5)
C(143)-C(101)-C(121)	108.4(5)
C(88)-C(102)-C(67)	120.4(5)
C(95)-C(103)-C(116)	111.4(5)
C(95)-C(103)-C(106)	105.5(4)
C(116)-C(103)-C(106)	111.2(5)
C(95)-C(103)-C(119)	109.1(5)
C(116)-C(103)-C(119)	111.1(5)
C(106)-C(103)-C(119)	108.3(5)
C(114)-C(104)-C(122)	119.5(6)
C(124)-C(105)-C(111)	119.7(6)
C(62)-C(106)-C(96)	118.0(5)

C(62)-C(106)-C(103)	117.7(5)
C(96)-C(106)-C(103)	124.1(5)
C(122)-C(107)-C(70)	121.4(6)
C(90)-C(108)-C(97)	121.3(5)
C(124)-C(109)-C(81)	121.4(6)
C(118)-C(110)-C(88)	119.1(5)
C(76)-C(111)-C(105)	118.1(5)
C(76)-C(111)-C(101)	118.3(5)
C(105)-C(111)-C(101)	123.5(5)
C(94)-C(112)-C(91)	119.7(5)
C(115)-C(113)-C(72)	119.5(6)
C(84)-C(114)-C(104)	119.9(6)
C(92)-C(115)-C(113)	119.4(6)
C(129)-C(117)-C(99)	121.2(6)
C(110)-C(118)-C(63)	120.6(5)
C(141)-C(120)-C(93)	119.8(6)
C(107)-C(122)-C(104)	119.7(6)
C(68)-C(123)-C(58)	121.5(5)
C(109)-C(124)-C(105)	119.9(5)
C(109)-C(124)-C(128)	120.8(6)
C(105)-C(124)-C(128)	119.4(6)
C(69)-C(125)-C(126)	121.3(6)
C(125)-C(126)-C(97)	118.9(6)
C(144)-C(127)-C(135)	121.7(7)
C(144)-C(127)-C(68)	111.8(7)
C(135)-C(127)-C(68)	112.0(6)
C(144)-C(127)-C(1)	99.1(7)
C(135)-C(127)-C(1)	101.8(7)
C(68)-C(127)-C(1)	108.3(6)
C(130)-C(128)-C(140)	101.4(12)
C(130)-C(128)-C(134)	108.8(9)
C(140)-C(128)-C(134)	114.8(12)
C(130)-C(128)-C(124)	108.2(6)
C(140)-C(128)-C(124)	112.0(7)
C(134)-C(128)-C(124)	111.0(7)
C(117)-C(129)-C(131)	119.3(6)

C(86)-C(131)-C(129)	118.8(6)
C(120)-C(141)-C(85)	119.6(6)
C(79)-C(142)-C(98)	119.4(5)
C(200)-C(201)-C(205)#2	119.1(11)
C(205)-C(206)-C(207)	114.2(12)
C(206)-C(205)-C(201)#3	118.0(12)
C(202)-C(203)-C(204)	149.9(19)

Symmetry transformations used to generate equivalent atoms:

#1 $-x, y, -z+1/2$ #2 $x, -y+1, z-1/2$ #3 $x, -y+1, z+1/2$

Table 4. Anisotropic displacement parameters ($\text{\AA}^2 \times 10^3$) for 04168t. The anisotropic displacement factor exponent takes the form: $-2\pi^2 [h^2 a^{*2} U^{11} + \dots + 2 h k a^* b^* U^{12}]$

	U^{11}	U^{22}	U^{33}	U^{23}	U^{13}	U^{12}
C(140)	238(17)	410(20)	58(7)	-81(11)	-11(9)	243(18)
C(1)	54(5)	117(8)	51(5)	-5(5)	11(4)	-25(5)
Pd(1)	27(1)	33(1)	21(1)	0	10(1)	0
P(7)	28(1)	36(1)	21(1)	-1(1)	10(1)	-2(1)
P(8)	35(1)	38(1)	25(1)	-1(1)	11(1)	7(1)
O(3)	39(2)	36(2)	25(2)	-5(2)	14(2)	-3(2)
C(3)	29(2)	32(3)	30(3)	2(2)	12(2)	1(2)
C(4)	51(3)	46(3)	26(3)	6(2)	16(2)	21(3)
C(5)	33(3)	42(3)	25(2)	5(2)	15(2)	1(2)
C(6)	37(3)	42(3)	24(2)	-5(2)	16(2)	-9(2)
C(7)	32(3)	46(3)	28(3)	-4(2)	9(2)	7(2)
C(8)	37(3)	37(3)	51(4)	-1(3)	22(3)	1(2)
C(9)	32(3)	54(4)	35(3)	-1(3)	6(2)	-5(3)
C(10)	45(3)	39(3)	35(3)	-11(2)	25(3)	-12(2)
C(11)	30(3)	50(3)	46(3)	-3(3)	17(3)	-7(2)
C(12)	35(3)	32(3)	26(2)	1(2)	10(2)	1(2)
C(13)	53(4)	39(3)	42(3)	-12(3)	30(3)	-5(3)
C(14)	30(3)	43(3)	44(3)	-2(3)	12(2)	1(2)
C(15)	36(3)	39(3)	36(3)	-9(2)	19(2)	0(2)
C(16)	39(3)	42(3)	22(2)	-9(2)	15(2)	-11(2)
C(17)	49(3)	44(3)	25(3)	-6(2)	18(2)	-16(3)
C(18)	34(3)	43(3)	34(3)	-3(2)	16(2)	-3(2)
C(19)	33(3)	37(3)	33(3)	-8(2)	14(2)	-1(2)
C(20)	36(3)	38(3)	43(3)	-4(2)	17(3)	5(2)
C(21)	36(3)	50(3)	24(2)	-7(2)	10(2)	10(2)
C(22)	51(3)	45(3)	33(3)	-10(2)	23(3)	-16(3)
C(23)	31(3)	41(3)	30(3)	-3(2)	7(2)	-2(2)
C(24)	39(3)	47(3)	41(3)	12(3)	16(3)	0(3)
C(25)	51(3)	55(4)	25(3)	-6(2)	16(3)	-22(3)
C(26)	37(3)	71(5)	44(4)	8(3)	8(3)	1(3)
C(27)	43(3)	54(4)	61(4)	-11(3)	32(3)	-11(3)

C(28)	40(3)	73(5)	46(4)	21(3)	13(3)	4(3)
C(29)	41(3)	61(4)	31(3)	10(3)	12(2)	1(3)
C(30)	61(4)	55(4)	20(3)	-5(2)	14(3)	-14(3)
C(31)	38(3)	42(3)	47(3)	-8(3)	22(3)	0(2)
C(32)	39(3)	86(5)	30(3)	13(3)	8(3)	-1(3)
C(33)	39(3)	60(4)	52(4)	18(3)	21(3)	14(3)
C(34)	45(4)	62(4)	58(4)	31(3)	17(3)	7(3)
C(35)	48(3)	37(3)	49(4)	-3(3)	24(3)	4(3)
C(36)	55(4)	71(5)	44(4)	22(3)	26(3)	23(3)
C(37)	37(3)	114(7)	28(3)	-11(4)	16(3)	4(4)
C(38)	95(6)	49(4)	26(3)	-1(3)	20(3)	9(4)
C(39)	77(5)	41(3)	52(4)	-15(3)	39(4)	-9(3)
C(40)	111(7)	62(5)	31(3)	5(3)	22(4)	10(5)
C(41)	75(5)	61(4)	41(4)	16(3)	26(4)	18(4)
C(42)	37(3)	67(5)	75(5)	-27(4)	-4(3)	22(3)
C(43)	39(4)	51(4)	85(6)	13(4)	7(4)	6(3)
C(44)	101(7)	87(6)	36(4)	-11(4)	30(4)	10(5)
C(45)	119(7)	64(5)	46(4)	10(4)	28(5)	-16(5)
C(46)	55(5)	181(11)	45(4)	16(6)	10(4)	-16(6)
C(47)	86(6)	43(4)	54(4)	-2(3)	-10(4)	-11(4)
C(48)	44(4)	91(6)	70(5)	-40(5)	3(4)	13(4)
C(49)	161(10)	47(4)	146(9)	22(5)	128(9)	19(5)
Pd(2)	22(1)	38(1)	16(1)	-2(1)	8(1)	0(1)
P(3)	25(1)	44(1)	17(1)	-1(1)	9(1)	4(1)
P(4)	24(1)	40(1)	17(1)	-2(1)	9(1)	1(1)
P(5)	24(1)	40(1)	16(1)	0(1)	9(1)	0(1)
P(6)	24(1)	42(1)	20(1)	-5(1)	9(1)	-2(1)
O(2)	25(2)	42(2)	24(2)	-1(2)	9(1)	4(2)
O(1)	31(2)	49(2)	19(2)	3(2)	12(1)	8(2)
C(52)	30(2)	38(3)	19(2)	0(2)	13(2)	0(2)
C(53)	21(2)	48(3)	19(2)	0(2)	7(2)	0(2)
C(54)	31(3)	43(3)	18(2)	1(2)	9(2)	1(2)
C(55)	24(2)	46(3)	20(2)	-5(2)	9(2)	7(2)
C(56)	32(3)	46(3)	20(2)	2(2)	12(2)	7(2)
C(57)	34(3)	51(3)	26(3)	-5(2)	14(2)	9(2)
C(58)	31(3)	49(3)	27(3)	4(2)	14(2)	5(2)

C(59)	29(2)	41(3)	24(2)	-6(2)	11(2)	1(2)
C(60)	29(2)	38(3)	15(2)	1(2)	7(2)	-2(2)
C(61)	23(2)	52(3)	23(2)	0(2)	10(2)	5(2)
C(62)	31(3)	47(3)	23(2)	2(2)	11(2)	8(2)
C(63)	29(2)	43(3)	22(2)	0(2)	11(2)	1(2)
C(64)	33(3)	52(3)	23(2)	-3(2)	12(2)	-7(2)
C(65)	26(2)	43(3)	22(2)	-3(2)	11(2)	-1(2)
C(66)	25(2)	48(3)	18(2)	3(2)	7(2)	4(2)
C(67)	22(2)	42(3)	21(2)	-1(2)	5(2)	-3(2)
C(68)	37(3)	77(5)	20(2)	2(3)	7(2)	12(3)
C(69)	26(2)	65(4)	20(2)	6(2)	6(2)	-3(2)
C(70)	34(3)	40(3)	23(2)	-6(2)	10(2)	-10(2)
C(71)	28(2)	43(3)	19(2)	-4(2)	12(2)	-1(2)
C(72)	31(3)	45(3)	26(3)	2(2)	11(2)	4(2)
C(73)	27(3)	58(4)	27(3)	2(2)	11(2)	5(2)
C(74)	29(3)	59(4)	22(2)	-1(2)	11(2)	2(2)
C(75)	29(3)	53(3)	21(2)	-5(2)	10(2)	3(2)
C(76)	30(3)	43(3)	32(3)	-8(2)	12(2)	1(2)
C(77)	38(3)	43(3)	23(2)	-3(2)	16(2)	-1(2)
C(78)	33(3)	49(3)	27(3)	0(2)	15(2)	6(2)
C(79)	29(3)	61(4)	35(3)	9(3)	16(2)	5(3)
C(80)	28(2)	46(3)	21(2)	4(2)	12(2)	3(2)
C(81)	28(3)	50(3)	26(2)	-8(2)	8(2)	3(2)
C(82)	28(2)	43(3)	23(2)	1(2)	12(2)	5(2)
C(83)	32(3)	49(3)	20(2)	-1(2)	8(2)	9(2)
C(84)	39(3)	48(3)	20(2)	-2(2)	11(2)	-3(2)
C(85)	41(3)	46(3)	37(3)	-3(3)	20(3)	-7(3)
C(86)	44(3)	50(3)	28(3)	-7(2)	12(2)	-9(3)
C(87)	35(3)	48(3)	20(2)	2(2)	7(2)	10(2)
C(88)	48(3)	44(3)	53(4)	-10(3)	26(3)	-15(3)
C(89)	38(3)	48(3)	33(3)	2(2)	9(2)	4(2)
C(90)	22(2)	47(3)	22(2)	6(2)	12(2)	0(2)
C(91)	31(3)	46(3)	29(3)	-9(2)	15(2)	-2(2)
C(92)	32(3)	58(4)	34(3)	-7(3)	16(2)	3(3)
C(93)	29(3)	45(3)	33(3)	-3(2)	13(2)	5(2)
C(94)	45(3)	47(3)	31(3)	-4(2)	23(3)	-6(3)

C(95)	39(3)	46(3)	24(2)	8(2)	15(2)	12(2)
C(96)	44(3)	62(4)	17(2)	2(2)	11(2)	16(3)
C(97)	27(3)	58(4)	51(4)	17(3)	14(3)	5(3)
C(98)	34(3)	57(4)	44(3)	6(3)	13(3)	2(3)
C(99)	46(3)	48(3)	23(2)	-5(2)	15(2)	6(3)
C(100)	38(3)	61(4)	23(3)	-1(3)	4(2)	8(3)
C(101)	34(3)	48(3)	39(3)	2(3)	10(2)	9(2)
C(102)	47(3)	37(3)	43(3)	-5(2)	25(3)	-3(2)
C(103)	38(3)	62(4)	26(3)	13(3)	19(2)	18(3)
C(104)	61(4)	66(4)	32(3)	-8(3)	24(3)	-24(3)
C(105)	38(3)	59(4)	47(4)	-14(3)	15(3)	6(3)
C(106)	41(3)	55(4)	21(2)	8(2)	15(2)	19(3)
C(107)	41(3)	76(5)	31(3)	-17(3)	19(3)	-21(3)
C(108)	29(3)	44(3)	39(3)	5(2)	15(2)	2(2)
C(109)	26(3)	60(4)	36(3)	-17(3)	6(2)	6(2)
C(110)	38(3)	50(3)	36(3)	0(3)	17(3)	-10(3)
C(111)	34(3)	47(3)	34(3)	-4(2)	10(2)	8(2)
C(112)	34(3)	53(3)	29(3)	-11(2)	16(2)	-3(2)
C(113)	34(3)	53(4)	36(3)	-3(3)	12(2)	-2(3)
C(114)	49(3)	56(4)	27(3)	-5(3)	15(3)	-4(3)
C(115)	31(3)	54(4)	36(3)	-10(3)	12(2)	1(2)
C(116)	58(4)	108(6)	27(3)	21(3)	28(3)	37(4)
C(117)	58(4)	59(4)	27(3)	-14(3)	21(3)	-2(3)
C(118)	35(3)	50(3)	25(2)	1(2)	14(2)	-2(2)
C(119)	53(4)	60(4)	56(4)	19(3)	34(3)	14(3)
C(120)	38(3)	45(3)	51(4)	-2(3)	16(3)	1(3)
C(121)	51(4)	51(4)	59(4)	11(3)	22(3)	1(3)
C(122)	54(4)	94(6)	32(3)	-19(3)	22(3)	-38(4)
C(123)	32(3)	60(4)	27(3)	4(3)	8(2)	9(3)
C(124)	35(3)	63(4)	53(4)	-24(3)	14(3)	6(3)
C(125)	33(3)	66(4)	28(3)	13(3)	8(2)	1(3)
C(126)	33(3)	72(5)	47(4)	21(3)	17(3)	1(3)
C(127)	46(4)	118(7)	27(3)	-6(4)	-7(3)	21(4)
C(128)	43(4)	92(6)	49(4)	-30(4)	7(3)	25(4)
C(129)	68(4)	54(4)	38(3)	-12(3)	23(3)	-9(3)
C(130)	209(13)	73(6)	240(15)	-73(8)	202(13)	-51(8)

C(131)	60(4)	62(4)	37(3)	-11(3)	18(3)	-14(3)
C(132)	52(4)	63(5)	68(5)	-14(4)	6(4)	2(4)
C(133)	46(4)	141(8)	37(4)	-30(5)	-7(3)	45(5)
C(134)	269(17)	63(6)	224(15)	-68(8)	210(15)	-51(9)
C(135)	57(5)	152(9)	38(4)	-33(5)	16(3)	-11(5)
C(137)	61(5)	123(8)	35(4)	29(4)	-1(3)	-2(5)
C(138)	207(14)	91(8)	590(30)	-173(14)	320(20)	-86(9)
C(139)	59(5)	211(12)	45(4)	-26(6)	3(4)	71(7)
C(141)	44(3)	43(3)	53(4)	3(3)	22(3)	0(3)
C(142)	34(3)	48(3)	43(3)	13(3)	12(3)	5(3)
C(143)	42(3)	58(4)	48(4)	4(3)	8(3)	18(3)
C(144)	29(4)	154(10)	77(6)	-39(6)	-8(4)	5(5)
C(145)	175(11)	284(17)	74(6)	100(9)	101(7)	183(12)

References

- For two recent reviews see: (a) Jiang, L.; Buchwald, S. L. *Metal-Catalyzed Cross-Coupling Reactions*, 2nd ed., Wiley-Interscience: Weinheim, 2004, 2, 699-760. (b) Hartwig, J. F. *Handbook of Organopalladium Chemistry for Organic Synthesis*, Negishi, E., Ed. Wiley-Interscience: Weinheim, 2002, 1051.
- Kranenburg, M.; van der Burgt, Y. E. M.; Kamer, P. C. J.; van Leeuwen, P. W. N. M. *Organometallics* **1995**, *14*, 3081.
- (a) Guari, Y.; van Es, D. S.; Reek, J. N. H.; Kamer, P. C. J.; van Leeuwen, P. W. N. M. *Tetrahedron Lett.* **1999**, *40*, 3789. (b) Harris, M. C.; Geis, O.; Buchwald, S. L. *J. Org. Chem.* **1999**, *64*, 6019. (c) Yang, B. H.; Buchwald, S. L. *Org. Lett.* **1999**, *1*, 35. (d) Wagaw, S.; Yang, B. H.; Buchwald, S. L. *J. Am. Chem. Soc.* **1999**, *121*, 10251. (e) Yin, J.; Buchwald, S. L. *Org. Lett.* **2000**, *2*, 1101. (f) Yin, J.; Buchwald, S. L. *J. Am. Chem. Soc.* **2002**, *124*, 6043. (g) Yin, J.; Zhao, M. M.; Huffman, M. A.; McNamara, J. M. *Org. Lett.* **2002**, *4*, 3481. (h) Ji, J.; Li, T.; Bunnelle, W. H. *Org. Lett.* **2003**, *5*, 4611. (i) Anderson, K. A.; Menez-Perez, M.; Priego, J.; Buchwald, S. L. *J. Org. Chem.* **2003**, *68*, 9563. (j) Cacchi, S.; Fabrizi, G.; Goggiamani, A.; Zappia, G. *Org. Lett.* **2001**, *3*, 2539. (k) Artamkina, G. A.; Sergeev, A. G.; Beletskaya, I. P. *Tetrahedron Lett.* **2001**, *42*, 4381. (l) Sergeev, A. G.; Artamkina, G. A.; Beletskaya, I. P. *Tetrahedron Lett.* **2003**, *44*, 4719. (m) Browning, R. G.; Mahmud, H.; Badarinarayana, V.; Lovely, C. J. *Tetrahedron Lett.* **2001**, *42*, 7155. (n) Anbazhagan, M.; Stephens, C. E.; Boykin, D. W. *Tetrahedron Lett.* **2002**, *43*, 4221. (o) Jean, L.; Rouden, J.; Maddaluno, J.; Lasne, M-C. *J. Org. Chem.* **2004**, *69*, 8893.
- Anderson, K. A.; Buchwald, S. L. Unpublished results.
- For Xantphos studies see: (a) Guari, Y.; van Strijdonck, G. P. F.; Boele, M. D. K.; Reek, J. N. H.; Kamer, P. C. J.; van Leeuwen, P. W. N. M. *Chem. Eur. J.* **2001**, *7*, 475. (b) Kamer, P. C. J.;

- Van Leeuwen, P. W. N. M.; Reek, J. N. H. *Acc. Chem. Res.* **2001**, *34*, 895. (c) Yin, J.; Buchwald, S. L. *J. Am. Chem. Soc.* **2002**, *124*, 6043.
6. Sadighi, J. P.; Harris, M. C.; Buchwald, S. L.; *Tetrahedron Lett.* **1998**, *39*, 5327.
7. Van der Veen, L. A.; Keeven, P. K.; Schoemaker, G. C.; Reek, J. N. H.; Kamer, P. C. J.; van Leeuwen, P. W. N. M.; Lutz, M.; Spek, A. L. *Organometallics* **2000**, *19*, 872.
8. (a) Singh, U. K.; Strieter, E. R.; Blackmond, D. G.; Buchwald, S. L. *J. Am. Chem. Soc.* **2002**, *124*, 14104. (b) Nielsen, L. P. C.; Stevenson, C. P.; Blackmond, D. G.; Jacobsen, E. N. *J. Am. Chem. Soc.* **2004**, *126*, 1360. (c) Streiter, E. R.; Blackmond, D. G.; Buchwald, S. L. *J. Am. Chem. Soc.* **2005**, *127*, 4120.
9. Toluene was used to make a stock solution of Xantphos so that a more accurate amount of Xantphos could be injected into the reaction vessel. Toluene was used rather than 1,4-dioxane due to solubility problems.
10. van der Veen, L. A.; Kamer, P. C. J.; van Leeuwen, P. W. N. M. *Angew. Chem. Int. Ed.* **1999**, *38*, 336.
11. Hayashi, T.; Konishi, M.; Kobori, Y.; Kumada, M.; Higuchi, T.; Hirotsu, K. *J. Am. Chem. Soc.* **1984**, *106*, 158.
12. (a) Brown, J. M.; Cooley, N. A. *Organometallics*, **1990**, *9*, 353. (b) Katz, T. J.; Garratt, P. J. *J. Am. Chem. Soc.* **1964**, *86*, 4876.
13. This is most likely the complex formed. It cannot be isolated, see experimental.
14. Care must be taken to keep the solution cold in the NMR tube before analysis, since this cyclooctatetraene complex decomposes upon warming.
15. The only other palladium(0) bix-xanthene crystal structure reported is Pd(ethylXantphos)₂ (in this case, it is diethylphosphines instead of diphenylphosphines on the xanthene backbone): Raebiger, J. W.; Miedaner, A.; Curtis, C. J.; Miller, S. M.; Anderson, O. P.; DuBois, D. L. *J. Am. Chem. Soc.* **2004**, *126*, 5502.
16. This solid can appear green if there is a small amount of palladium black present.
17. Sanford, M. S.; Love, Jennifer, A.; Grubbs, R. H. *J. Am. Chem. Soc.* **2001**, *123*, 6543.

Liane M. Klingensmith

402 Highland Ave. #20
Somerville, MA 02144

Phone (Home): (857) 998-0249
Email: Klingensmith@gmail.com

OBJECTIVE

A pharmaceutical research and development position utilizing my experience in metal-catalyzed cross-coupling reactions, mechanistic studies, and synthetic organic chemistry.

EDUCATION

Master of Science, Massachusetts Institute of Technology, Cambridge, MA August 2003-June 2005
Concentration: Organic Chemistry Advisor: Professor Stephen L. Buchwald
Research Area: Mechanistic studies on palladium-catalyzed carbon-nitrogen bond formation

Bachelor of Arts, *summa cum laude*, Alfred University, Alfred, NY August 1999-May 2003
Major: Chemistry, Concentration: Organic (graduated with honors)
Minor: Mathematics, Concentration: Topology

PROFESSIONAL EXPERIENCE

Graduate Research Assistant August 2003-present
Massachusetts Institute of Technology, Cambridge, MA Advisor: Professor Stephen L. Buchwald

- Performed mechanistic studies on carbon-nitrogen bond forming reactions
- Synthesized phosphine ligands and organometallic species for use in organic synthesis

Graduate Teaching Assistant Spring 2005 and 2004, Fall 2003
Massachusetts Institute of Technology, Cambridge, MA Courses: Advanced Organic Chemistry
Laboratory Chemistry

- Held regular recitation sessions and office hours, graded

Undergraduate Research Assistant August 2002-May 2003
Alfred University, Alfred, NY Advisor: Dr. Andrew Eklund

- Performed kinetic studies of ring-closing metathesis reactions using gas chromatography

Research Assistant May 2002-August 2002
King's College London, London, England Advisor: Dr. Nicholas Leadbeater

- Used mechanochemical grinding to enhance the performance of Suzuki reactions
- Discovered and developed "ligand-free", solvent-less, room temperature conditions for a wide variety of Suzuki substrates

NSF-REU Undergraduate Research Assistant June 2001-August 2002
Northwestern University, Evanston, IL Advisor: Professor Eric Weitz

- Studied the effect of a zeolite environment on the photolysis of trifluoroacetone with UV radiation

PUBLICATIONS

Klingensmith, Liane M.; Leadbeater, Nicholas E. "Ligand-free palladium catalysis of aryl coupling reactions facilitated by grinding" *Tetrahedron Letters* **2003**, 44(4), 765-768.

Klingensmith, Liane M.; Strieter, Eric R.; Buchwald, Stephen L. "Identification of Pd Speciation During the Pd-Catalyzed C-N Bond-Forming Reaction Using Catalysts Based on Xantphos" in preparation.

AWARDS

Alfred University Outstanding Senior Finalist 2003, ACS Corning Section Outstanding Senior Award 2003, Phi Kappa Phi Award of Excellence 2003, Outstanding Performance in Organic Chemistry 2001, CRC Freshman Chemistry Achievement Award 2000